

DISTRIBUTION OF SONORAN PRONGHORN (*ANTILOCAPRA AMERICANA  
SONORIENSIS*) ON AN ACTIVE AIR FORCE TACTICAL RANGE

by

Samuel C. Price

A Thesis Presented to the  
FACULTY OF THE USC GRADUATE SCHOOL  
UNIVERSITY OF SOUTHERN CALIFORNIA  
In Partial Fulfillment of the  
Requirements for the Degree  
MASTER OF SCIENCE  
(GEOGRAPHIC INFORMATION SCIENCE AND TECHNOLOGY)

May 2015

Copyright 2015

Samuel C. Price

## **DEDICATION**

I dedicate this document to my parents for their continuous encouragement throughout my education, and to my fiancé for her sacrifice of time, and her dealing with a grouchy and tired me.

## **ACKNOWLEDGMENTS**

I thank my supervisor Nicole Tautfest for helping and recommending ideas while planning the early stages of this project. I also thank those up at Luke AFB who agreed to let me use these data for my thesis, specifically Aaron Alvidrez, whom I was in contact with. Much thanks as well to my advisor, Dr. Travis Longcore, for being patient with my ever-changing schedule.

**TABLE OF CONTENTS**

DEDICATION	ii
ACKNOWLEDGMENTS	iii
LIST OF TABLES	vi
LIST OF FIGURES	vii
LIST OF ABBREVIATIONS	x
ABSTRACT	xi
CHAPTER 1: INTRODUCTION	1
CHAPTER 2: RELATED WORK	4
2.1 Sonoran Pronghorn	4
2.2 Areas of Intensive use by Sonoran Pronghorn	7
2.2.1 Kernel Density Estimation	7
2.2.2 Hotspots	9
2.3 Maximum Entropy Modelling	10
CHAPTER 3: METHODS	13
3.1 Study Area	13
3.2 Data Collection	14
3.3 Data Analysis	16
3.3.1 Hotspots	17
3.3.2 Maximum Entropy Modelling	18
3.3.2.1 Layer Preparation	18
3.3.2.2 Maxent Settings	21

CHAPTER 4: RESULTS	27
4.1 Hotspots	28
4.2 Maximum Entropy Modelling	39
CHAPTER 5: CONCLUSION AND DISCUSSION	48
REFERENCES	52
APPENDIX A: HOTSPOT MAPS	59
APPENDIX B: SEASONAL HOTSPOT DISTANCE TABLE	75

**LIST OF TABLES**

Table 1 Annual SPH Population Estimates and Maximum Individuals per Range	4
Table 2 Annual Hotspots' Distance to Nearest Target	32
Table 3 Percent Contribution of Variables in the Two Model Runs	43
Table 4 Model Comparison of AUC and Standard Deviation Values	47
Table 5 Seasonal Hotspots' Distance to Nearest Target	75

## LIST OF FIGURES

Figure 1 SPH at water/feed station; male (back), fawns (front-left), and female (right) - Photograph by USFWS Remote Camera.....	5
Figure 2 NTAC and STAC Study Area on the BMGR East.....	14
Figure 3 Monitoring From One of the Observation Points (OP Echo).....	16
Figure 4 Euclidean Distance Calculation for the Target Feature Class in ArcMap 10.1.....	20
Figure 5 Maxent Main Page.....	22
Figure 6 Basic Settings Choices for Maxent.....	24
Figure 7 Advanced Settings Choices for Maxent .....	25
Figure 8 Study Area With All SPH Sightings Displayed Over Targets and Roads .....	27
Figure 9 Fawning Season 2013 Hotspot Location Map with Underlying KDE and Overlaid with a Distance from Nearest Target Table .....	28
Figure 10 Summer Season 2013 Hotspot Location Map with Underlying KDE and Overlaid with a Distance from Nearest Target Table .....	29
Figure 11 Breeding Season 2013 Hotspot Location Map with Underlying KDE and Overlaid with a Distance from Nearest Target Table .....	30
Figure 12 Hotspot Locations for the Entire Year of 2013 with Underlying KDE and Overlaid with a Distance from Nearest Target Table .....	31
Figure 13 Boxplot for Seasonal Variation in Hotspot Distance from Nearest Target .....	33
Figure 14 Annual Hotspots from 2010-2013 Above 1KM Target Buffer .....	35
Figure 15 Seasonal Hotspots for 2010.....	35
Figure 16 Seasonal Hotspots for 2011 .....	36
Figure 17 Seasonal Hotspots for 2012.....	37

Figure 18 Seasonal Hotspots for 2013 .....	38
Figure 19 Average AUC for 1,000 Replicates Including the Wetness Index .....	40
Figure 20 Variable Response Curves for 1,000 Replicates Including the Wetness Index. From Left to Right the Variables Shown Include Observer Distance, Distance from Road, Slope, Distance from Target, and Wetness Index.....	40
Figure 21 Jackknife Test on AUCs for 1,000 Replicates Including the Wetness Index. From Top to Bottom, the Environmental Variables Include, Observer Distance, Distance from Roads, Slope, Distance from Targets, and Wetness Index .....	41
Figure 22 Average AUC for 1,000 Replicates with the Wetness Index Removed.....	42
Figure 23 Jackknife Test on AUCs for 1,000 Replicates with the Wetness Index Removed. From Top to Bottom, the Environmental Variables Include Observer Distance, Distance from Roads, Slope, and Distance from Targets .....	42
Figure 24 Predictive Output Raster from the Second Model, Showing Probability of a Sighting.....	44
Figure 25 Average AUC for 1,000 Replicates Using All Sightings with the 25 Percent Subsample Statistical Method.....	45
Figure 26 Predictive Output Raster from the Third Model, Showing Probability of a Sighting.....	46
Figure 27 SPH 2010 Hotspot Map with Underlying KDE Raster .....	59
Figure 28 SPH 2010 Breeding Season Hotspot Map with Underlying KDE Raster .....	60
Figure 29 SPH 2010 Fawning Season Hotspot Map with Underlying KDE Raster.....	61
Figure 30 SPH 2010 Summer Season Hotspot Map with Underlying KDE Raster .....	62
Figure 31 SPH 2011 Hotspot Map with Underlying KDE Raster .....	63

Figure 32 SPH 2011 Breeding Season Hotspot Map with Underlying KDE Raster .....	64
Figure 33 SPH 2011 Fawning Season Hotspot Map with Underlying KDE Raster.....	65
Figure 34 SPH 2011 Summer Season Hotspot Map with Underlying KDE Raster .....	66
Figure 35 SPH 2012 Hotspot Map with Underlying KDE Raster .....	67
Figure 36 SPH 2012 Breeding Season Hotspot Map with Underlying KDE Raster .....	68
Figure 37 SPH 2012 Fawning Season Hotspot Map with Underlying KDE Raster.....	69
Figure 38 SPH 2012 Summer Season Hotspot Map with Underlying KDE Raster .....	70
Figure 39 SPH 2013 Hotspot Map with Underlying KDE Raster .....	71
Figure 40 SPH 2013 Breeding Season Hotspot Map with Underlying KDE Raster .....	72
Figure 41 SPH 2013 Fawning Season Hotspot Map with Underlying KDE Raster.....	73
Figure 42 SPH 2013 Summer Season Hotspot Map with Underlying KDE Raster .....	74

**LIST OF ABBREVIATIONS**

AFB	Air Force Base
ANOVA	Analysis of Variance
AUC	Area Under the Curve
BMGR	Barry M. Goldwater Range
DEM	Digital Elevation Model
GIS	Geographic Information System
GME	Geospatial Modeling Environment
KDE	Kernel Density Estimate
MGRS	Military Grid Reference System
NTAC	North Tactical Range
ROCC	Range Operations Control Center
SPH	Sonoran Pronghorn
STAC	South Tactical Range
US	United States
USAF	United States Air Force
USFWS	United States Fish and Wildlife Service

## ABSTRACT

The population of Sonoran pronghorn (SPH; *Antilocapra americana sonoriensis*), an endangered subspecies within the United States (US), has fluctuated from an estimated 282 individuals in 1994 to 21 in 2002 and back up to over 150 as of August 2014. As the population continues to recover from drought-associated stressors, more SPH frequent the Barry M. Goldwater military tactical range and the United States Air Force (USAF) closes more targets from training for longer periods of time. In this thesis, hotspot analyses are combined with maximum entropy distribution modeling to understand the geographic and seasonal variation in SPH distribution at North and South Tactical Ranges (NTAC, STAC) in the Barry M. Goldwater Range East, Arizona using data from a monitoring effort begun in 1997.

Results show hotspots of high densities of SPH near strafing and bombing targets, supporting previous studies using fewer data. In Maxent-derived habitat models, distance from targets had the strongest effect on model performance, followed by slope of the ground. According to the models, distance from roads had no effect on the SPH locations, nor did distance from observer. Prior studies attribute SPH preference for areas near targets to attractiveness of forb growth following disturbance as forage, and high visibility resulting from few tall shrubs or bushes. Output from the distribution model provides a predictive map of habitat use that can be used to evaluate effects of range use on SPH in the future.

## CHAPTER 1: INTRODUCTION

Sonoran pronghorn (*Antilocapra americana sonoriensis*) is an endangered subspecies of pronghorn that frequents an active Air Force tactical range in Southwestern Arizona. The primary conservation effort is to increase the population size through captive breeding and protection from military and recreational activities. Current SPH habitat encompasses approximately 20,000 square kilometers on the Barry M. Goldwater Range (BMGR), Cabeza Prieta National Wildlife Refuge and the Organ Pipe Cactus National Monument (Krausman et al. 2005b). In 2011, a re-introduction effort expanded the range into the King's Valley of Kofa National Wildlife Refuge (USFWS 2010). Consistently, 20-45 SPH utilize the BMRG range, which is a heavily used training range for the Air Force and Marines. Since 2005, no analyses have been undertaken of the data collected to examine continued trends. Using new spatial analysis tools I can examine the data and compare it with prior studies' results. Hotspot analyses and maximum entropy modelling were used to describe range areas with high densities of use and to identify potential variables important in predicting the species' future use. Detailed information regarding their spatial behavior in this habitat will both help the military plan future training missions and will additionally enhance biologists' ability to understand the subspecies.

The goal of this project was to assess where SPH are most likely to occur during different portions of the year, potentially allowing the USAF to plan missions by focusing on areas of lesser predicted use during particular time periods. This was accomplished through the use of hotspots, using core use areas of a kernel density estimate to define each location (Blundell et al. 2001; Wal & Rodgers 2012). To examine why SPH preferred their observed locations, maximum entropy modelling of distributions was applied to the sightings, using a number of environmental variables (Phillips et al. 2004, 2006). The output of these models both define important variables,

and predict the probability of observing a SPH in a particular location. To accomplish these goals, two related questions are asked. First, where in the study area are SPH frequenting, and how does it change between seasons and between years? The answer to this question shows where SPH were seen during a certain time period, though it does not answer why they were there. This introduces the second question, what characteristics of the study area are important in defining and predicting SPH location choice? These results showed what variables have high predictive value when trying to determine future use by SPH.

Historically, SPH existed in the Sonoran desert of Mexico, up into southwestern Arizona and as far west as southeastern California (O’Gara 1978). The United States Fish and Wildlife Service (USFWS) listed SPH as endangered in 1967 (USFWS 1998; deVos and Miller 2005). Since then, the population within the United States (US) has fluctuated due to drought from an estimated 282 individuals in 1994, to fewer than 30 individuals in 2002 (Morgart et al. 2005; Krausman et al. 2005a). The current population estimate is approximately 300 individuals within the US. From a purely scientific basis, this limited population warrants special attention and analysis.

SPH utilize all areas of the North (NTAC) and South Tactical Ranges (STAC) on the BMGR in Southwestern Arizona, including areas directly surrounding live fire and high explosive targets (Krausman et al. 2005b). Missions occur almost daily, including low, dry overflights as well as actual releasing of bullets towards targets, and bombs towards high explosive hills.

Studies have shown that this subspecies of pronghorn has a mean individual home-range size of 511 km<sup>2</sup> with ranges between 43-2873 km<sup>2</sup> (Hervert et al. 2005). Habitat preferences within this tactical range have been described, showing that pronghorn presence is mostly evenly

distributed throughout vegetation types, though there is a significant preference for disturbed areas including both targets and burned patches (Krausman et al. 2005b). Between 1997 and 2005, the population in the study area was quite low, and steadily decreasing. Since 2005, no in-depth analyses have updated the results from these studies, or examined changes in range use as the population increased.

As the population continues to recover, and more SPH frequent the tactical ranges, the USAF is required to close down a greater number of targets for longer periods of time. Current operating instructions require normal targets to be shut down for a period of 24 hours following a pronghorn sighting within a one-kilometer buffer. For high explosive targets, this buffer is extended to 1.5 km. In a study area of between 10 – 25 km from West to East, and approximately 30 km North to South, a large area is often shut down during portions of the year because of multiple, widespread sightings of SPH groups and individuals.

This study provides additional information to the range managers about areas of high density use by SPH throughout the year. Perhaps target use priorities can be identified for different times of the year. While predicting target use throughout the year will not change target closures, mission planning can be made more efficient by focusing on historically less active targets for a specific time period. Also, in the event of new target complexes being developed, areas of low use can be chosen for target placement. Examining use of the ranges by SPH is providing information about the effects of targets, roads and other variables on SPH movement and area use.

## CHAPTER 2: RELATED WORK

The SPH are one of five subspecies of pronghorn in the US (Hosack et al. 2002; Krausman et al. 2005a). The sizes of the two remaining US and Mexico populations of SPH are estimated every other year (Table 1; ie. Mexico in 2012, US in 2013), a process that began in 2000 and continues to present time (Pronghorn recovery meeting, 2013). Until 2002, the population was declining sharply, with few sightings in the study area, though since then it has increased almost every consecutive year (Table 1). Both populations are unstable, with little genetic diversity due to the genetic bottleneck (Stephen et al. 2005). The majority of written work on SPH resides in technical documents, though a few exist in peer reviewed journal articles as well as a number of book sections (Krausman et al. 2005c). Most of these published articles or books refer to data collected prior to 2003, with one or two as recent as 2005.

**Table 1 Annual SPH Population Estimates and Maximum Individuals per Range**

Year (20xx)	00	01	02	03	04	05	06	07	08	09	10	11	12	13
Max # on NTAC	16	15	13	8	6	9	4	6	13	27	24	24	23	40
Max # on STAC	14	21	13	9	9	6	23	20	25	26	41	32	19	44
Max Total on Range	16	21	16	10	13	9	23	20	25	31	45	43	42	57
Population Estimate	<b>100</b>	-	<b>21</b>	-	<b>58</b>	-	<b>68</b>	-	<b>68</b>	-	<b>85</b>	-	<b>159</b>	-

*Source:* Data provided by USFWS and Nicole Taufest at Chiulista Services, Inc.

### 2.1 Sonoran Pronghorn

Pronghorn are a small deer-like ungulate living throughout parts of North America. Of the five subspecies, the SPH is the rarest, existing in three separate populations in southwestern Arizona and in northwestern Mexico (Stephen et al. 2005; Mottsinger 2013). Adapted to dry conditions, this subspecies is somewhat smaller and lighter than the other North American subspecies, with a

maximum weight between 48–60 kilograms (105-133 lbs). Because of widely distributed food sources and drier conditions, home-ranges of the SPH are much larger than the other subspecies (Yoakum 1978), at an average of 511 km<sup>2</sup>, compared to 22–170 km<sup>2</sup> of pronghorn from other areas of the United States (Hervert et al. 2005). SPH have a characteristic sandy brown body, with white stripes on the neck and a white belly and chest (Figure 1; Reid 2006). Males have a distinct black patch behind the cheek.



**Figure 1 SPH at water/feed station; male (back), fawns (front-left), and female (right) -**

**Photograph by USFWS Remote Camera**

SPH prefer habitat dominated by palo verde (*Parkinsonia* spp) and chain fruit cholla cactus (*Opuntia fulgida*), in part because the cholla fruit provides a source of stored water (Fox 1997). In years of high precipitation, creosote-bursage habitat communities are frequented, as

herbaceous plants grow abundantly (Hervert et al. 2005). Diet consists dominantly of forbs and grasses, which are taken advantage of soon after precipitation, or in disturbed areas. Some succulent shrubs are consumed during the winter months where forbs have been consumed or have died out (Ochenfels 2014). Currently, hay is provided to supplement natural food sources in captive pens and near artificial water sources in an effort to minimize mortality from starvation.

For many years it was thought that SPH required little to no freestanding water for drinking, deriving all needed moisture from food sources (Tinker 1978). In 1987, a SPH was photographed drinking from an artificial water source, and since then multiple similar sightings have been documented using wildlife cameras (Morgart et al. 2005). Freestanding water is important to SPH, and severe droughts limited water and forage, helping to cause the decline to an estimated 21 individuals in the US by 2002 (Bright & Hervert 2005).

Observations of SPH on NTAC and STAC (the study area for this thesis) from 1999–2002 indicate that approximately 73 percent of sightings occurred in military disturbed areas (Krausman et al. 2005b). In a similar report, Hervert et al. (1997) demonstrated SPH were attracted to target areas because they could see predators at a greater distance across the open desert landscape, as well as the access to standing water and forb growth resulting from constant disturbance. Another study focusing on the soil surrounding high explosive targets found that standing water in bomb craters was most likely of limited use to SPH because of the high rates of evapotranspiration (Tetra Tech 2005). This same study found that residue left by explosions added insignificant amounts of sodium to the landscape, so it is unlikely the SPH are attracted due to the conditions being similar to a salt lick. In general, little difference in SPH behavior were observed on the BMGR between 1998-2000, when anthropogenic noise levels were increased by aircraft (Krausman et al. 2001). For adult SPH, behavior changed less than 50

percent of the time. The conclusions drawn by Krausman, Harris, and Francine (2001) are that military activities have minimal effects on SPH when appropriate monitoring and target closures are in effect.

## **2.2 Areas of Intensive use by Sonoran Pronghorn**

Hotspots are defined as spatial clusters of points (Liu and Brown 2003). These clusters are areas with a high density of features or phenomena of interest (Nelson and Boots 2008). While a number of methods are available to calculate and analyze hotspots, local spatial autocorrelation and kernel estimators are the two most often used tools. Kernel estimators create density surfaces, the highest values of which are distinguished as hotspots. Often these density surfaces are used to define overall distributions, or home ranges and core use areas of animals (Kie et al. 2010; Worton 1989). For this thesis, only the core use areas were used when defining hotspots, because highest use is the primary interest.

### ***2.2.1 Kernel Density Estimation***

Kernel density estimation (KDE) is applied to many fields of study, including but not limited to medicine (Er et al. 2010), invasive species outbreaks (Nelson and Boots 2008), crime analysis (Liu and Brown 2003), home-range studies (Blundell et al. 2001), and evaluation of hazardous conditions (Mola-Yudego and Gritten 2010; Lin et al. 2011). A KDE creates a continuous raster density surface over a two-dimensional XY coordinate plane (Downs and Horner 2008; Xie and Yan 2008; Downs 2010). This density surface is useful for visualizing locations of spatial abundance, as well as emphasizing areas with a lack of use. Because density is represented in this way, not only are the focus points of abundance obvious, but a visible and calculable relationship between spatial location and likelihood of an occurrence happening is established (Anderson 2009).

When creating a KDE from a set of locations, two primary variables greatly affect the output raster: the bandwidth (search radius/threshold) and the output cell size (Nelson and Boots 2008; Anderson et al. 2009; Krisp and Peters 2011). The bandwidth represents the search radius of the kernel calculation while searching for nearby points. This variable is represented by a distance chosen manually as a fixed kernel, or automatically as an adaptive kernel (Seaman and Powell 2005). Larger bandwidth values produce smoother and larger KDE area calculations (Ramp et al. 2005). The output cell size does not affect the calculation as much as the output visualization grid. Cell size is the pixel size representation of the KDE (Nelson and Boots 2008). Cell size should not be smaller than the minimum point accuracy being input into the KDE. To create an accurate density estimation, Seaman et al. (1999) recommends the use of at minimum 30 geographic locations, and ideally 50 or more.

Fixed kernels for a KDE are chosen manually, relying on the judgment of the researcher. Wand and Jones (1995) describe this method by examining various bandwidth values from largest to smallest, and finding the one that is “most pleasing” to the researcher. This method is subjective, allowing the researcher to decide how smooth the edges of the raster output will be. For example, an edge with little smoothing has sharper edges, conforming more closely to the actual input points while a smoother edge will incorporate more area, with fewer to no sharp corners. Nelson and Boots (2008), studying mountain pine beetle hotspots, recommend using values between 800–2000 meters because they return results that are smoothed, but not so smoothed as to overestimate the distributions. A fixed kernel method may be useful when the study purpose involves data exploration for hypotheses before another analysis (Silverman 1986).

Adaptive kernels are those that allow for local variation in smoothing of density calculations. This means that areas of lower density are smoothed differently than those with higher densities because of their nearness to other points (Wand and Jones 1995). While these are useful in many situations, such as when working with data that are unknown to the researcher, the approach has drawbacks. The main drawback is that comparability between samples is lost because the local variation is calculating different results across the range, instead of using a known, and comparable, search radius.

### ***2.2.2 Hotspots***

Kernel estimated hotspots are used for many types of analyses, both on a two dimensional plane, and across a network. Nelson and Boots (2008) used KDE methods to locate hotspots of mountain pine beetle infestations. They examined bandwidth values of 450, 800, 2000, and 9500 meters, and found that the middle two were best because they did not create as many fine scale unconnected hotspots, nor as many large, over connected hotspots. Lin et al. (2011) examined soil pollution hotspots using KDE methods and found it an appropriate method of delineating areas of high pollution. A KDE output shows density of geographic location, and when these densities are combined with geostatistics they show variables of interest within the attribute table that coincide with those spatial densities. Anderson (2009) and Xie and Yan (2008) both investigated traffic incident hotspots with KDEs. Anderson found that the continuous surface of a KDE was useful in providing a spread of risk, showing predictive values at locations nearby but not on top of known incidents. Xie and Yan (2008) took a standard KDE method and adapted it for a network, concluding that their method was an improvement over the standard when using a road network. In the wildlife and ecological field, hotspots are often used to examine road mortality of animals, as is the case for a study by Ramp et al (2005), looking at fatalities along

the Snowy Mountain Highway in Australia. For this study, a bandwidth of 500 meters was chosen a priori to be comparable with nearby analyses. Ramp et al. (2005) concluded that spatial clustering using density is an appropriate method for identifying hotspots.

### **2.3 Maximum Entropy Modelling**

Maximum entropy modelling is a method of distribution modelling using presence-only data (Phillips, Dudik, and Schapire 2004; Elith et al. 2011). This method is useful because even though an observer does not see an animal at a sample location, it may be hiding, or visibility may be less than ideal, which introduces observer bias (Gu and Swihart 2004). In addition, absence data are often not available, either because they were not collected, or because a project did not have enough funding to sample enough sites to accurately or sufficiently delineate absence locations. This modelling method evaluates the most uniform distribution across an area, which allows the model to show how much better the data fit than a uniform distribution would (Baldwin 2009). Though relatively new, this tool has been used extensively, with over one thousand publications since 2006 (Merow, Smith, and Silander 2013).

Maxent is a software package designed to analyze data in this way, looking at environmental variables to distinguish possible relationships between the location of animals and the contributing variables (Phillips, Dudik, and Schapire 2004). This software allows a user to input location points for a species or multiple species of interest, in a comma delimited file (CSV), using three columns: "Species," "X," and "Y." Environmental variables, which are any potentially contributing variables, must be included in an ASCII format, and must be cropped to the exact spatial dimensions. Many settings and tests can be specified within the options, including the input feature method, the output format, and statistical calculations performed.

Although Maxent has many benefits, such as the ability to perform well with very limited sample sizes, Hernandez et al. (2006) point out that model accuracy increases for smaller geographic ranges, and for species with more restricted environmental tolerance. The potential for sampling bias can negatively affect the usability of the results as well, though this is the case in most studies dealing with wildlife. When choosing environmental variables for a particular model, care should be taken to select variables that correspond well with the geographic locations of the species. For example, an average precipitation layer should be from the same temporal scale as that of the points being analyzed. Similarly, variables with little variation across the study area extent should not be used, as they will not affect the model because they are not at the appropriate scale (Phillips, Anderson, and Schapire 2006).

The ability to perform accurate analyses of distributions with only presence data has made this method popular among the scientific community. Yost et al. (2008) used Maxent to map sage grouse nesting habitat in southern Oregon. They tested their models by withholding 25 percent of their data from the training algorithm. They found that the type of vegetation was most important in predicting nest sites, and visually, the output image of high probability areas were accurate when comparing with the nest sites withheld for testing.

Suarez-Seoane et al. (2008) used Maxent to analyze seasonal change in little bustard (*Tetrax tetrax*) distribution. They found that during the winter, lower elevations and more wastelands were occupied, which differed from the spring use of higher elevation pasturelands. The results showed that managers could potentially use spring habitat selection to predict winter habitat, which is important when managing a rare species, or a sport hunted species.

Also, a study on predictive modeling of microhabitat for endemic Chilean birds, by Moreno et al. (2011), used Maxent in a small geographic area (approximately 4.5 km<sup>2</sup>). They

showed one species' preference for areas farther from roads in lower elevation forest, while another species preferred higher percent slopes in more rugged terrain. Their study concludes that when combining GIS to visualize and produce results for the analysis, maximum entropy is a useful tool for forest management.

## CHAPTER 3: METHODS

This chapter introduces the methods used for this thesis. First, the study area is defined more clearly, then the data collection is explained. Because data collection started in 1997, some new tools have been introduced, though the methods remain similar. The data analysis techniques are described, beginning with the creation of hotspots, progressing to the use of Maxent to create distribution models. The Maxent methods include management and creation of layers to work within the software, and covers the settings used in this project.

### 3.1 Study Area

The data collected for this thesis come from NTAC and STAC, which are air-to-ground tactical ranges on the BMGR East (Figure 2). NTAC and STAC consist of 777 km<sup>2</sup> of mostly flat land with 813 individual targets that are combined into approximately 30 target complexes (USAF Targets 2013 dataset). Three of these complexes consist of high explosive targets, which are of extra concern and require more attention when monitoring. Bladed dirt and sand roads connect targets to each other for access and maintenance. Four primary observation points designed to provide the best coverage of all targets are used, and six secondary observation points are available for special use when necessary. Bordering the study area on the South and Southeast side is the Cabeza Prieta National Wildlife Refuge, and to the east is State Route 85, connecting Gila Bend, Arizona to Ajo, Arizona.

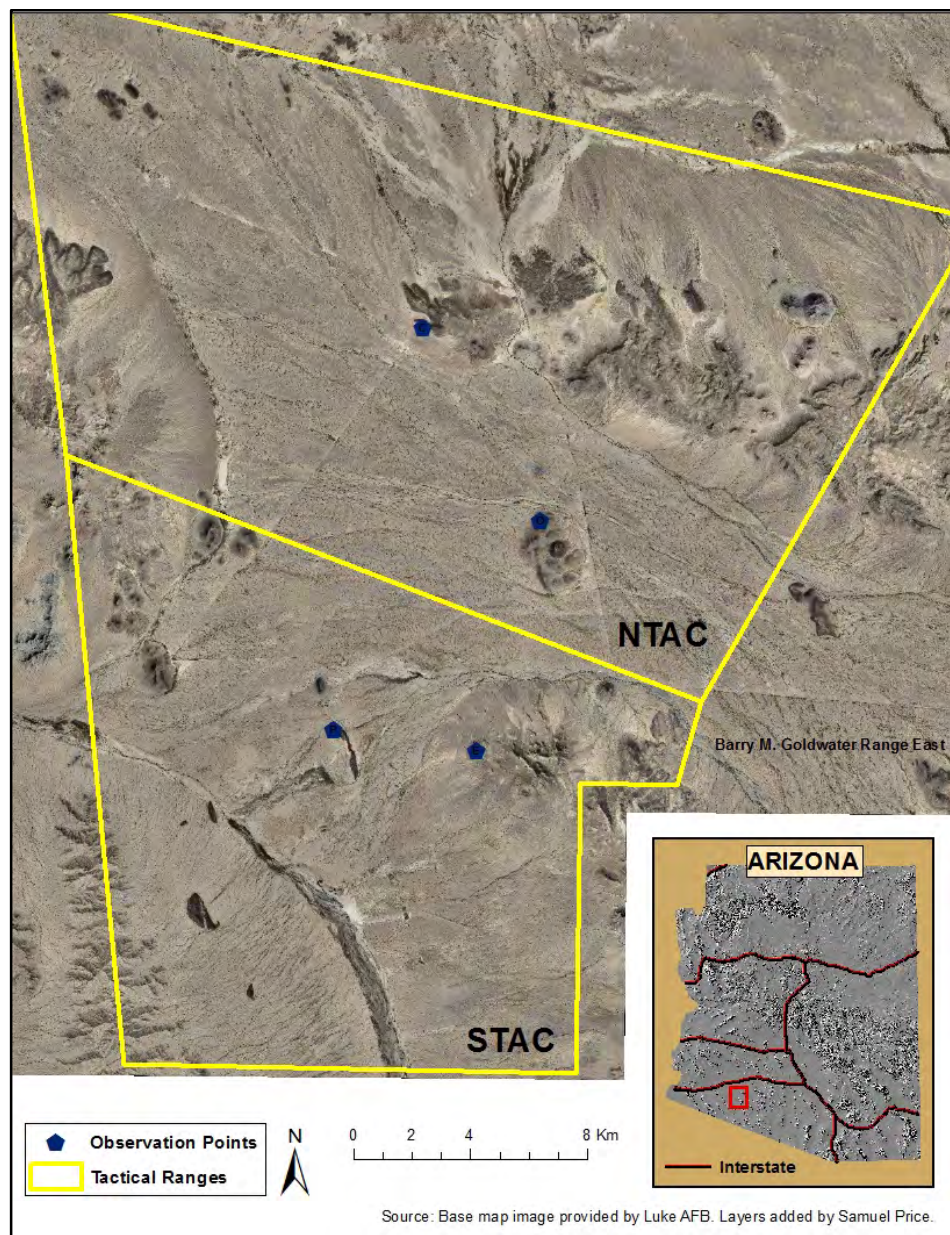


**Figure 2 NTAC and STAC Study Area on the BMGR East**

### 3.2 Data Collection

Data were collected from February 1997 to April 2014 and continue to be collected as part of an ongoing effort by the USAF to prevent SPH mortality caused by training activities in the study area. Certain operating procedures have changed over the years; however most of the changes pertain to buffer distances surrounding targets, which are closed from target practice following a

SPH sighting. Also, from 1997–2007, monitoring sessions were performed twice, rather than once, in a 24-hour period (Nicole Tautfest, face-to-face, December, 2014). The second monitoring session was primarily for double-checking the high explosive hills.

These methods are reported from the monitoring protocol set forth by the USAF and pronghorn biologists for monitoring SPH on the ranges (Pronghorn Biologists 2012). Starting at sunrise, biological monitors scan NTAC and STAC for at least two hours from primary observation points on each day with training missions (a minimum of two monitors on each range). When missions are late and monitoring is more difficult due to many animals or difficult environmental conditions, monitoring may go longer than the minimum two hours. Secondary observation points are used when one range is closed for maintenance, or when road or weather conditions limit access to the primaries.

Observation point locations were selected because they provided vantage points to see target complexes clearly, so SPH sightings are potentially biased towards locations near targets. Scanning is performed using 10x50 binoculars of various brands, as well as with 20-60x Leica and Swarovski spotting scopes (Figure 3). Scans of the target areas are prioritized over areas without targets, although surrounding areas are always scanned. In addition, telemetry is used to locate radio collared individuals across the landscape and to place them within visible groups. Yagi antennas (Communication Specialists, Orange, CA, USA) are used in combination with Communication Specialists (Orange, CA, USA) R-1000 receivers. A minimum of two crossing bearings is required for a location to be established by telemetry alone.

When a SPH or group of SPH is observed, location is recorded in military grid reference system (MGRS) format to the nearest 100 meters (e.g. TA946997). Basic behavioral observations are recorded, taking note of number of SPH in the group, sex, age, and general

direction of travel. At the end of the monitoring window, locations are reported to the range operations control center (ROCC), where they are input into ArcMap to determine target closures. Targets where inert ammunition is used are closed for a period of 24 hours if the sighting is within a one kilometer buffer. For the three high explosive target complexes, this buffer is extended to 1.5 kilometers.



**Figure 3 Monitoring From One of the Observation Points (OP Echo)**

### **3.3 Data Analysis**

All analyses were conducted using a combination of ArcMap (version 10.1), Geographic Modelling Environment (GME; version 0.7.2.1), R (version 3.1.0), and Maxent (version 3.3.3k). GME works as a standalone program, though it requires an installation of ArcGIS and R to function. It replaces an older ArcGIS plugin called “Hawths Tools,” which was created for ArcGIS 9.3.x, and specifically designed for advanced spatial analysis and modeling. Maxent is a standalone software package developed to study geographic distributions of species and to

predict probability of presence (Phillips, Anderson, and Schapire 2006; Phillips, Dudik, and Schapire 2006; Kumar and Stohlgren 2009).

### ***3.3.1 Hotspots***

This section prepares to answer the first question presented in this thesis: where are hotspots of SPH use across the study area? There is a temporal aspect within the question, in that variation occurring between seasons and throughout the year is important. For example, if biologists are wanting to predict SPH use during the month of November, they must examine a hotspot analysis of recent sightings and one from the previous year's coinciding time period. In this way, they will account for prior year's areas of high use while incorporating the current year's trends to predict important points within the study area for the future time period of interest. To achieve this task, hotspots were calculated for the years 2010-2014, and for each breeding, fawning, and summer season within each of those years. This was accomplished using ArcMap 10.1, creating a KDE with 100-meter cell size and a bandwidth of 1,000 meters. The bandwidth value was chosen because it represents the buffer distance for the majority of the targets throughout the range. Points within that distance of each other are important when calculating the density, and will be significant to the monitoring effort. Only time periods with a minimum of 30 sighting locations were used for the analysis, as recommended by Seaman et al. (1999). GME was then used to create polygons around the highest 20 percent of the density values. These polygons were brought back into ArcMap, and center points within each polygon were distinguished using the Feature to Point tool, specifying inside features. These were output into a new feature class named for the time period and sighting type (e.g. All SPH, year 2013 = cent\_2013). The visualizations were symbolized using large red or green dots over the KDE raster.

Hotspots were calculated for many different temporal scales, to examine variation at different times of the year, and between years. One hotspot map was produced for all sightings, one for each year's sightings, and one for each season from 2010-2014. For this analysis and the others, seasons are defined as: breeding season (Oct-Jan), fawning season (Feb-May), and summer season (Jun-Sep). Once calculated, these hotspots were put into a table and the distance from the nearest target was added. Both the annual hotspot table and the seasonal hotspot table were then analyzed using an analysis of variance (ANOVA) test using R, to test for significant differences in distance from nearest targets between years and between seasons.

### ***3.3.2 Maximum Entropy Modelling***

Maxent is a small but powerful program, with many features that are constantly being updated. These options allow users to customize the input features, as well as output formats and statistical analyses. Though customization is good for researchers with a good understanding of the methods involved, the default settings also produce accurate and usable results (Phillips and Dudik 2008; Baldwin 2009). Many of the following methods were derived from a tutorial (Phillips 2005).

#### ***3.3.2.1 Layer Preparation***

The first step in initiating this analysis consisted of preparing a plan to address the potential sampling bias inherent in any study. Creating an effort layer to use as a bias file within Maxent was not feasible because the only way to do so was very subjective. Therefore, the SPH dataset was split into two. The first dataset consisted only of telemetry sightings. These sightings were not visible to the observer's eyes, relying solely on telemetry bearings for previously radio collared SPH, and as such cannot be misplaced due to bad judgment of distance, or other visibility related environmental variables such as wind or haze and heat distortion. The second

dataset was created using only visual sightings, those seen without any telemetry aid. In this way, instead of setting aside a percentage of the overall sightings for training and testing, I created the telemetry layer for training the algorithms, and the visual layer for testing of that algorithm.

Next, I assembled and created the environmental layers. Though I accounted for some potential bias in observer ability by using telemetry sightings for training, I created a distance raster of distance from observation point to test the overall contribution of observation distance to sighting location. I created this layer using the Euclidean Distance tool within ArcMap, using 100 meter cell sizes. The 100 meter cell size was chosen because it coincides with the scale of the SPH sightings collected. Smaller sizes would potentially introduce artifacts, while larger sizes would limit the accuracy and utility of the output when considering such a small study area. This layer was called “Observer Distance.”

As distance from roads and distance from targets are considered important because of their inherent cause of disturbance to the SPH, I created a distance layer for each of these factors, with 100 meter cell size. Two layers were created, again using the Euclidean Distance tool in ArcMap, one from the target feature class, and one from the road feature class (Figure 4). Output raster layers were labeled “Target Distance,” and “Road Distance.”

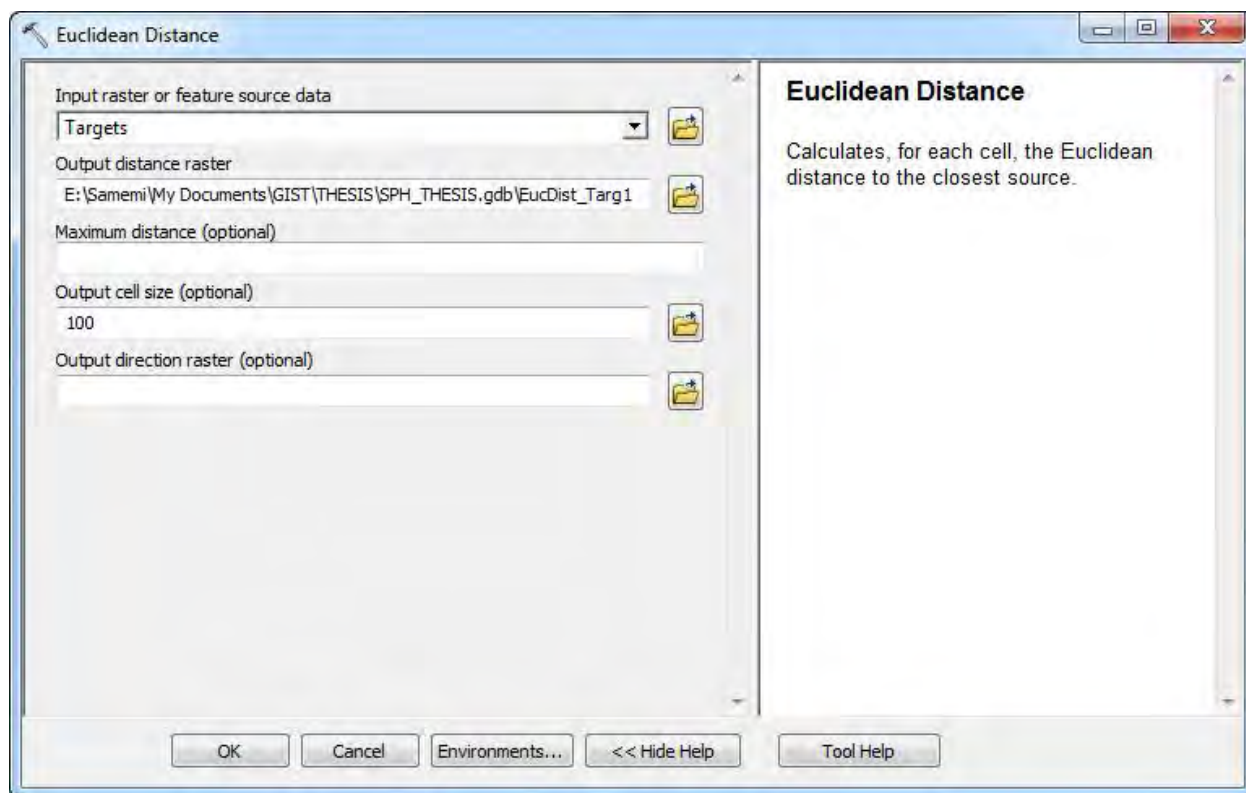


**Figure 4 Euclidean Distance Calculation for the Target Feature Class in ArcMap 10.1**

Observation of SPH show they prefer areas of flat ground, rarely venturing up slopes (Nicole Tautfest, face-to-face, July, 2014). Because access to some locations requires climbing hills or small mountains, it is not always the case that steep slopes are avoided. Because of this, I created a slope layer from a 90 meter Arizona digital elevation model (DEM), which was provided by biologists at Luke Air Force Base (AFB). I cropped the DEM to the general area, ran the Slope calculation tool within ArcMap, then resampled the raster to 100 meter cell sizes. This layer was named “Slope.”

Lastly, I created a wetness index layer, to see if soil water content had an effect on SPH location preference. A precipitation layer could be used, though because variation across such a small area is often quite low, the wetness index allows the study to look at overall drainage and

water storage rather than amount of precipitation directly. This layer was called “Wetness Index.”

To make sure each layer had the same geographic bounds, I created an extent layer, which I proceeded to use when clipping all the environmental layers to the same size. I clipped both input SPH layers as well, to make sure the overall extents matched. Once clipped, each layer was exported to ASCII format, using the Raster to ASCII tool for raster layers, and the Export Feature Attribute to ASCII for the SPH point features. The two SPH feature classes were organized into a single folder, while each raster layer and coinciding ASCII file were put into another folder, as required by Maxent.

### ***3.3.2.2 Maxent Settings***

The main screen for Maxent is relatively simple, though without reading through the tutorial and the descriptive papers on the software, choosing options would be quite complicated (Figure 5). On the top left, the samples used for the analysis are chosen from a single comma delimited file. Multiple species or groupings can be included in a single file, but in this case only one was needed. For my analysis, this was the telemetry only file. The top right of the screen is where the user must choose the folder containing the environmental layers, and then differentiate between each layer being of a continuous or categorical type. All of the environmental variables in this model were continuous.

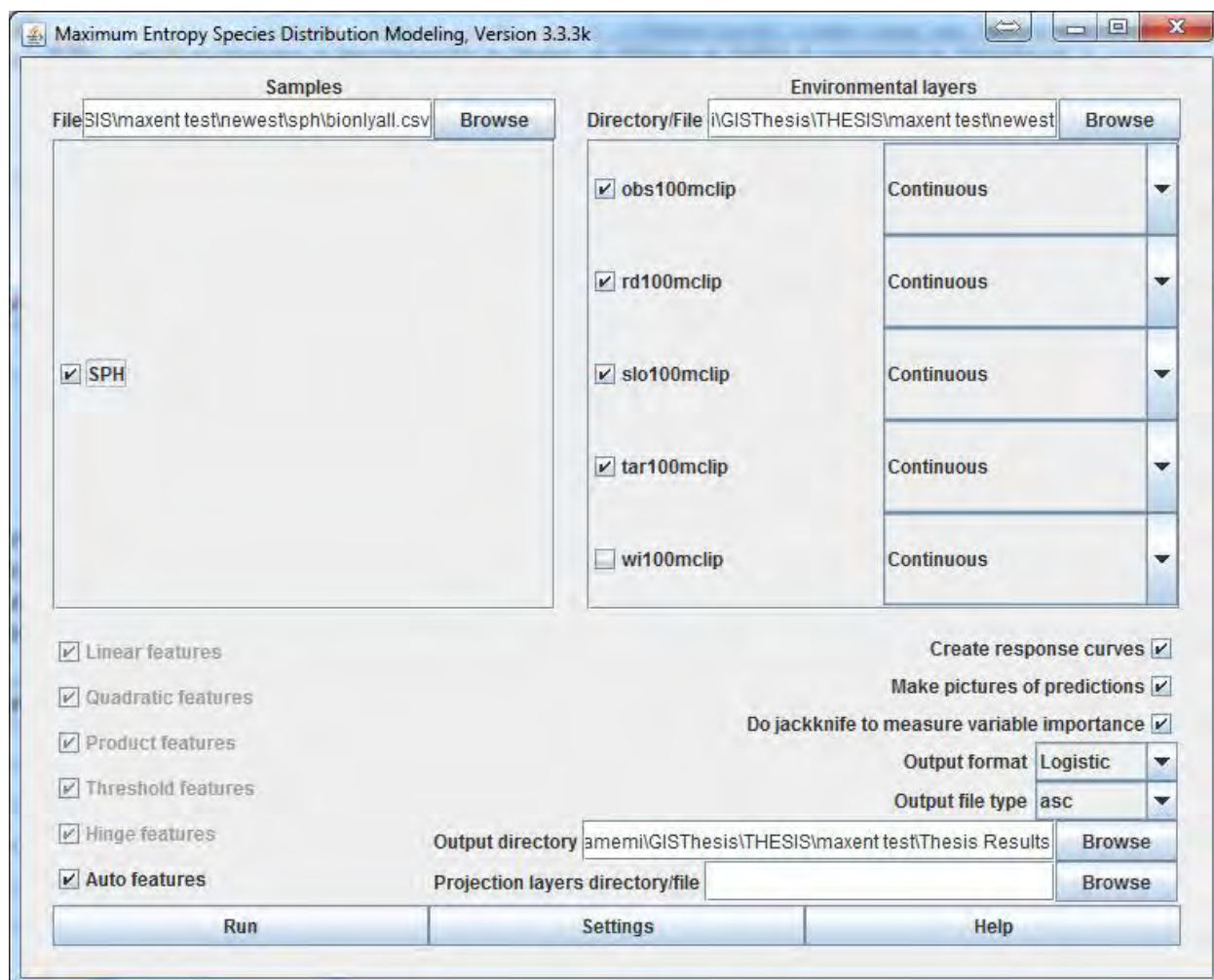


**Figure 5 Maxent Main Page**

Maxent has many options for features that vary the complexity of the model (Figure 5). The default setting is Auto, which lets the software choose the feature type based on the input variables. Merow, Smith, and Silander (2013) explain that when auto is checked, if there are more than 80 presence locations, then all the feature classes will be used. These features define how the model will be fit. I accepted the default of Auto, because it would run all of the feature types, choosing those that are most useful when building the model.

Underneath the environmental layers box, on the right, are check boxes to create response curves, picture predictions, and do jackknife tests to measure variable importance within the

model. Response curves show how input environmental variables affect the model prediction (Phillips 2005). The pictures of predictions creates an image of the output grid in a format easily readable by standard image viewers, in case access to ArcMap is limited. The Jackknife test examines variable importance to the overall model, by removing the variable and running the model again, to see the overall difference in results. In this way, a variable is assigned an importance to the model in the form of a percent contribution.

An output format of logistic was chosen because it produces a value within cells across the study area consistent with the probability of having a sighting at that location. It is easily understandable and provides a predictive capacity (Phillips, Anderson, and Schapire 2006; Phillips and Dudik 2008; Elith et al. 2011). I chose an output type of asc, for its ability to be incorporated into ArcMap for integration with future sighting information. Finally, I chose an output folder, which included all the output information produced during a model run.

After the main settings are chosen, clicking on the settings tab at the bottom brings up a new window with additional options (Figure 6). This is the page that allowed me to specify a test dataset of visual only sightings. When filling this, and specifying a test dataset, all sightings from the previous page's sighting input is used to train the model algorithm. Most options were left as default, except I increased the maximum number of background points from 10,000 to 20,000. Merow, Smith and Silander (2013) mention that the default or similar value is acceptable for this if all areas within the extent are potentially accessible to the species. I chose a larger maximum background points because of the large number of presence locations available (Phillip and Dudik 2008). Below that, I chose to run 1,000 replicates for statistical purposes, with crossvalidate as the replicated run type. This method leaves out "folds" of data, which are used

for testing against each other, providing evaluation for the model. In this way, it utilizes all the available data for testing each replicate run (Phillips 2005).

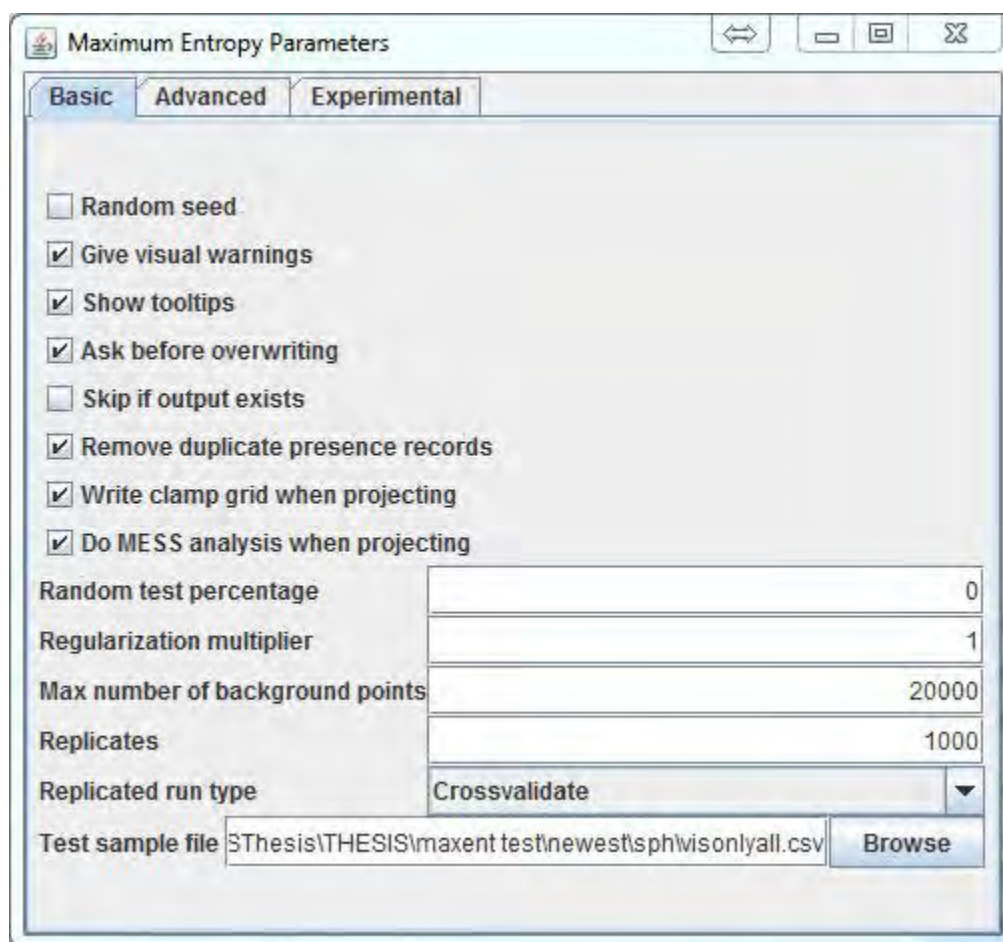


**Figure 6 Basic Settings Choices for Maxent**

Clicking to the right of the basic tab brings up the advanced options (Figure 7). All defaults were accepted except with an additional check mark for the “Write plot data” box, to provide access to raw data used in creating the response curves, in a format importable to peripheral software. After checking these settings, closing the window brings back the main page, where the run button can be clicked to start the analysis.

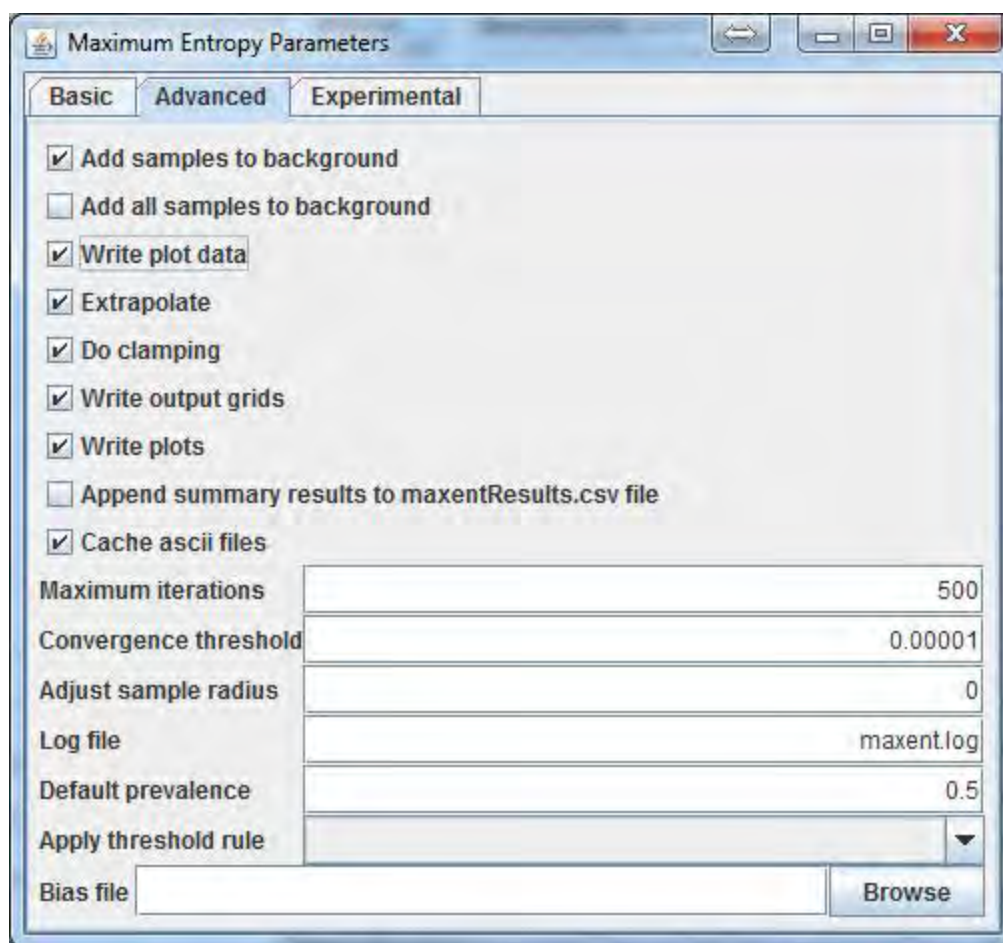


**Figure 7 Advanced Settings Choices for Maxent**

After these main analyses were completed, I ran three more models using mostly the same settings, except a more traditional approach to calculating statistics on the replicated runs. In the third model, I used all the data for SPH, combining all telemetry and visual sightings. Rather than cross-validation, I used the subsample feature which holds back a random percentage, in this case 25 percent, of points for testing, and the remaining 75 percent is for algorithm training. This model run is indicative of an ideal dataset with all points being equal in quality, with little to no observer bias. It was then compared to the model created to account for observer bias. The fourth model consisted of the same settings, but run on telemetry only sightings. The fifth model again used the same settings, but on the visual only sightings. These

last two models were run to see if there were any differences in model performance when the training and testing data were from one type of sighting, instead of both like model three, or separate for models one and two.

## CHAPTER 4: RESULTS

The analysis included 8,092 SPH sightings between March 1997 and March 2014 (Figure 8). The telemetry only sightings numbered 1,464 and visual only sightings were 3,919. The remaining 2,709 sightings were seen and located with telemetry, with no information as to whether they were seen before an animal with telemetry was heard, or whether the telemetry assisted in the observation. Because of this, these sightings were not used for the Maxent portion of the analysis, though they were all included when creating hotspots.

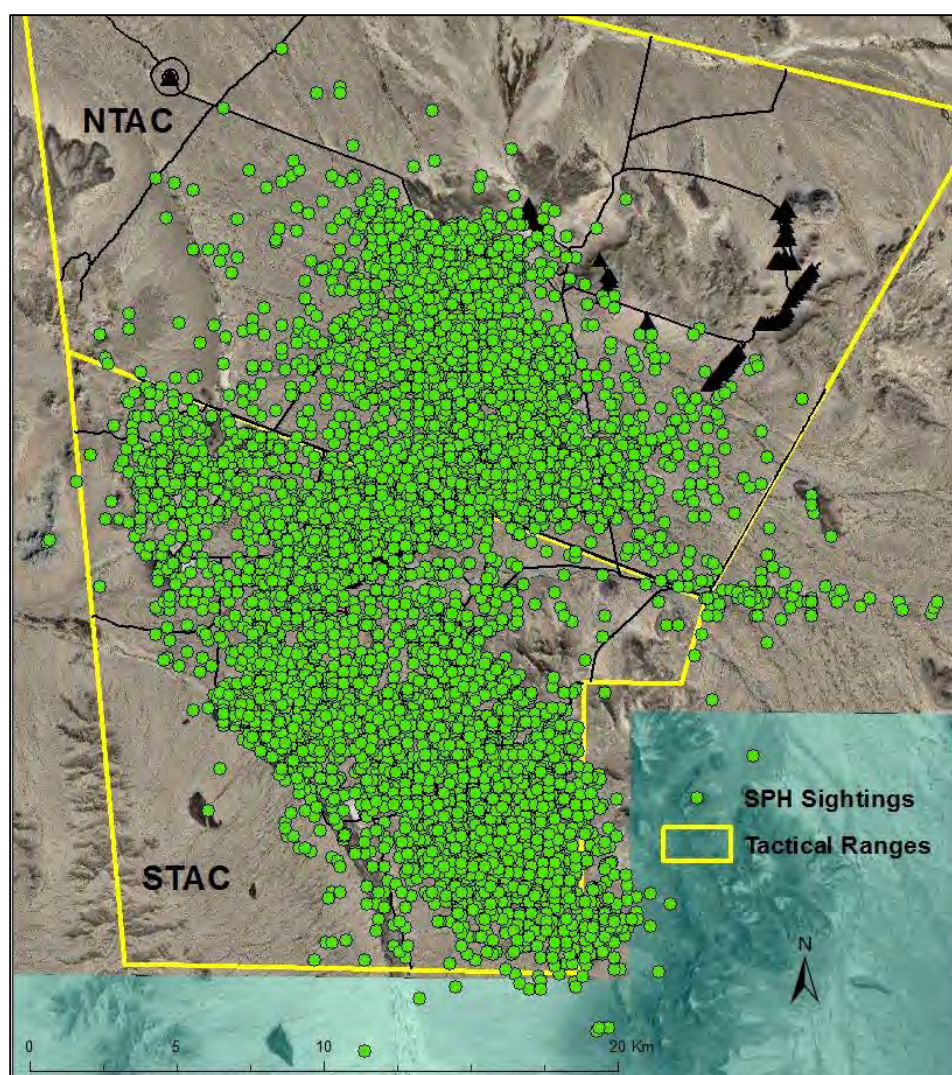


**Figure 8 Study Area With All SPH Sightings Displayed Over Targets and Roads**

## 4.1 Hotspots

Hotspot calculations using the 100-meter cell size and 1,000-meter bandwidth produced acceptable results that correspond visually with the locations of SPH sightings. Results are visually appealing, and portray the important details of high-density areas. To provide an example of the KDE output, a figure is shown of the KDE raster with isopleth polylines as well as hotspot locations (Figure 9). For all consecutive maps, only the hotspot locations are shown, along with coordinates for those locations and distance from nearest target. For the 2013 fawning season, the average distance from target was 466 meters. Ten of the eleven hotspots were <615 meters from targets, while a single hotspot was at 2.1 kilometers.

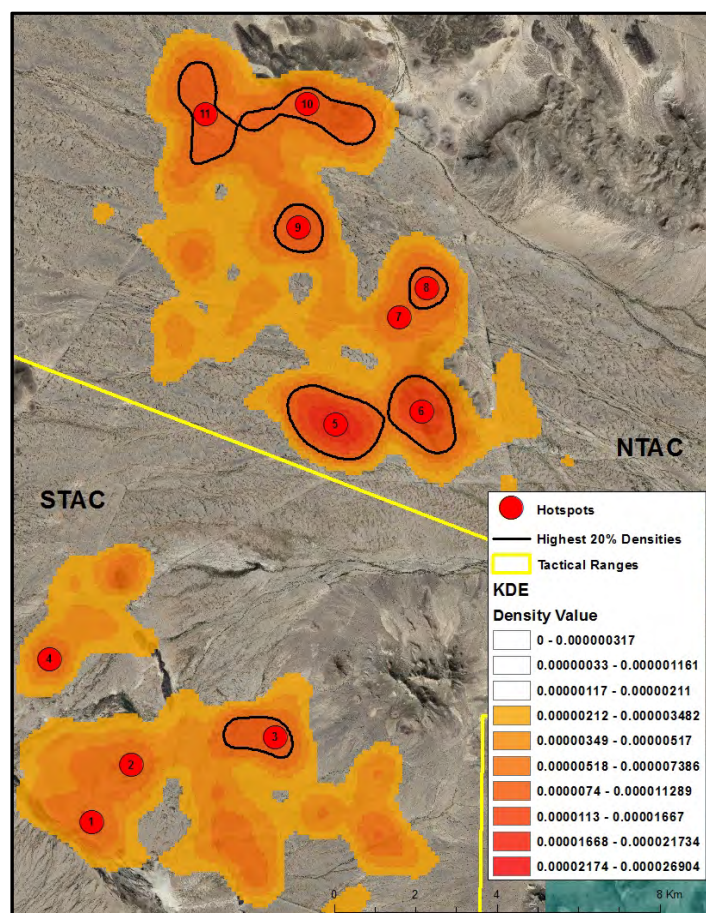


**Figure 9 Fawning Season 2013 Hotspot Location Map with Underlying KDE and Overlaid with a Distance from Nearest Target Table**

Summer and breeding season sample maps show similar hotspots, though the summer season map has hotspots located further south, towards the artificial water station (Figure 10, Figure 11). In the summer season, the average distance from targets was 1,127 meters, though six of the seven points were <670 meters, and one was at almost five kilometers. This farthest distance hotspot coincides with an artificial water and feed station, which is heavily used during the summer months, or other seasons during a dry year. The breeding season hotspots had an average distance of 317 meters to the nearest target, and the farthest was 600 meters.

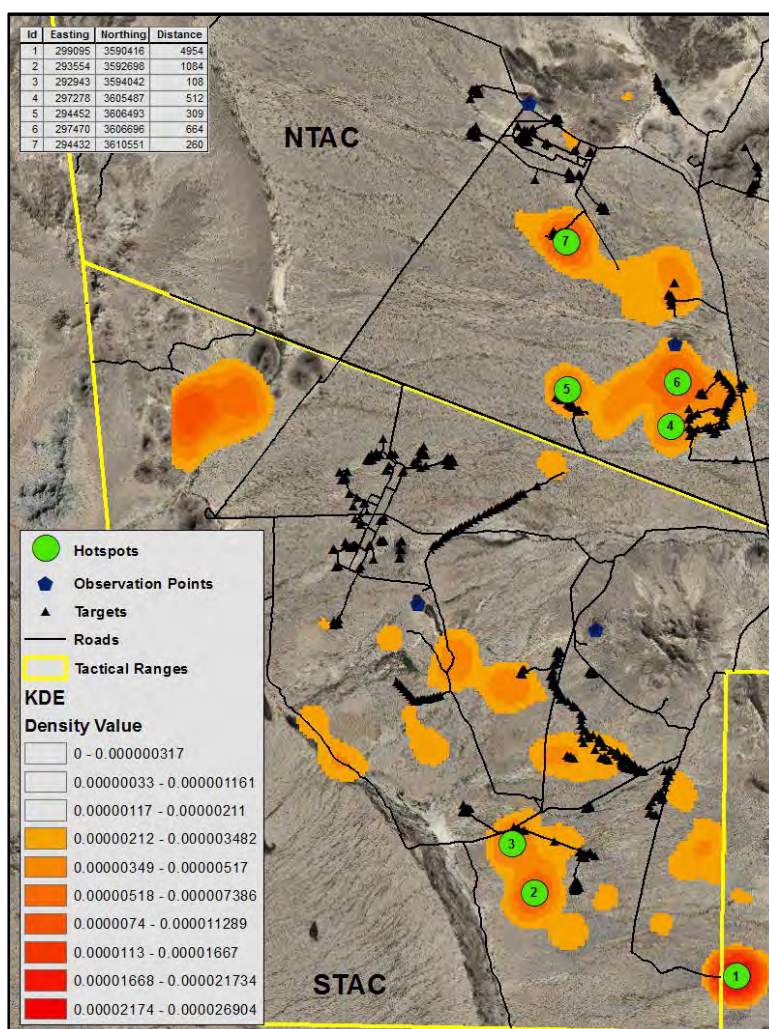


**Figure 10 Summer Season 2013 Hotspot Location Map with Underlying KDE and Overlaid with a Distance from Nearest Target Table**

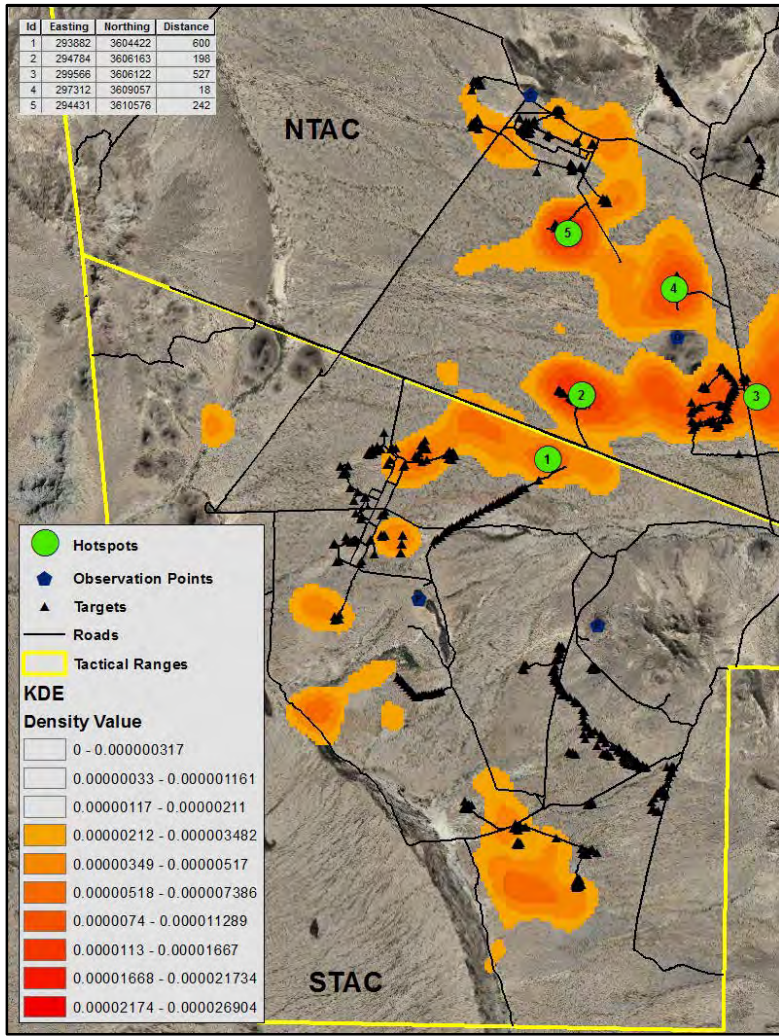


**Figure 11 Breeding Season 2013 Hotspot Location Map with Underlying KDE and Overlaid with a Distance from Nearest Target Table**

When taken as a whole, the 2013 sightings have hotspots in similar locations, though spread out over the entire area, rather than clumped in one part of the study area as are certain seasons. Looking at annual hotspots for 2013, few of them are different from any of the seasonal breakdown maps, they are just spread out over the entire area rather than clumped (Figure 12). Over the year, the average hotspot distance from a target comes to 1,254 meters, with four of the six locations under 1000 meters, one at 1,092 meters, and the farthest at five kilometers. Again,

this farthest location is at an artificial feeding station, which draws the SPH to it during hot and dry times of the year (location 1).

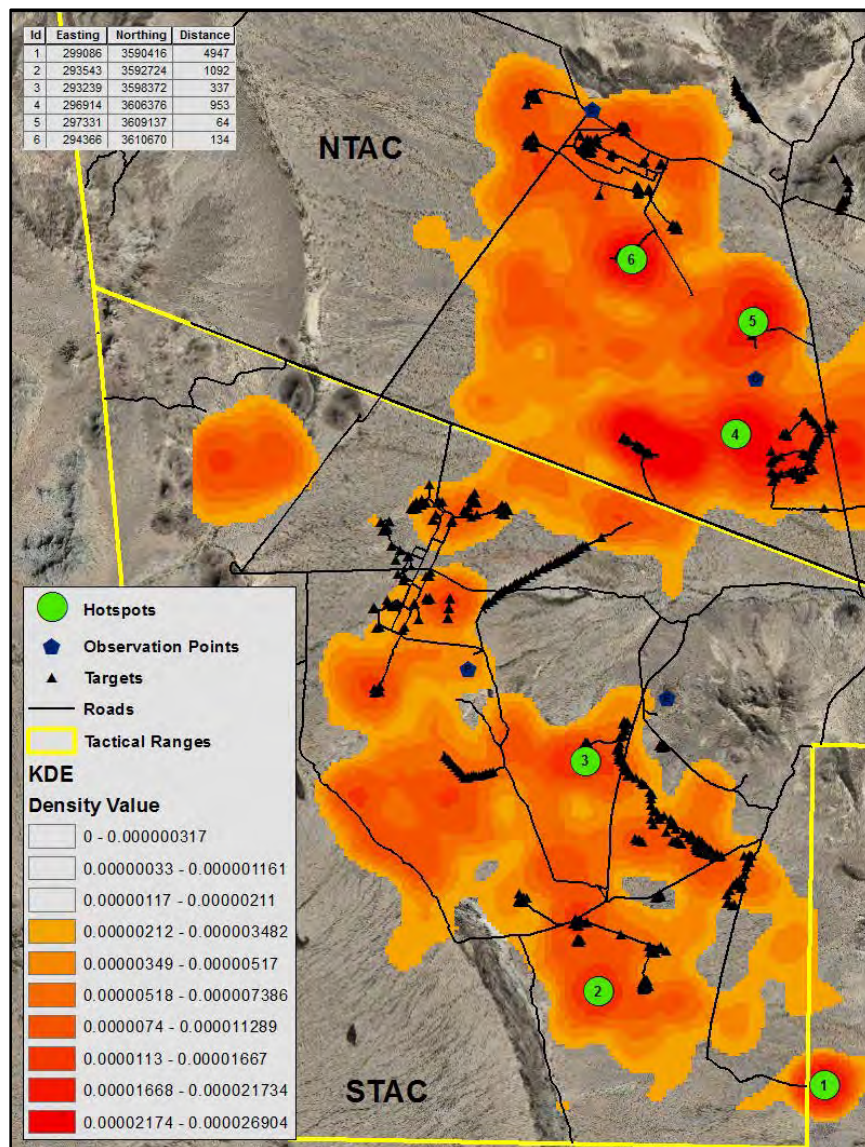


**Figure 12 Hotspot Locations for the Entire Year of 2013 with Underlying KDE and Overlaid with a Distance from Nearest Target Table**

A summary of hotspot distances emphasizes the nearness of these high use locations to targets. Annual hotspots are comprised of the entire year's SPH sightings, so must be tested separately from the seasonal hotspots, which split the locations into groups. Using an analysis of

variance (ANOVA) on the annual hotspots' distance from targets, there is no significant difference between years ( $F=0.006$ ,  $p=0.999$ ). There is an average of 1,305 meters from the nearest target, with a range of 36–5016 meters (Table 3). Each year has one large distance, near the artificial water source, and when this location is removed from each year, the average decreases to 388 meters.

**Table 2 Annual Hotspots' Distance to Nearest Target**

<u>Year</u>	<u>Hotspot</u>	<u>Distance</u>
2010	1*	4959
2010	2	737
2010	3	504
2010	4	316
2010	5	306
2011	1*	5016
2011	2	36
2011	3	341
2011	4	162
2012	1*	4980
2012	2	36
2012	3	332
2012	4	685
2012	5	171
2013	1*	4947
2013	2	1092
2013	3	337
2013	4	953
2013	5	64
2013	6	134

\*Located at artificial food and water station.

Seasonal hotspots show a different pattern, where there is a significant difference between the distance from targets during the summer season from the breeding and fawning seasons ( $F=3.978$ ,  $p=0.0236$ , Table 5-Appendix B). When the food and water station hotspots are removed from the data, the difference in target distance between seasons becomes insignificant

( $F=0.266$ ,  $p=0.7674$ ). The breeding seasons have an average distance from nearest target of 459 meters, while the fawning and summer season are 380 meters and 1,227 meters respectively. The summer season's average distance is much greater because of the artificial water source drawing SPH, and when these outliers are removed, the average distance to targets for the summer season decreases to 477 meters (Figure 13).

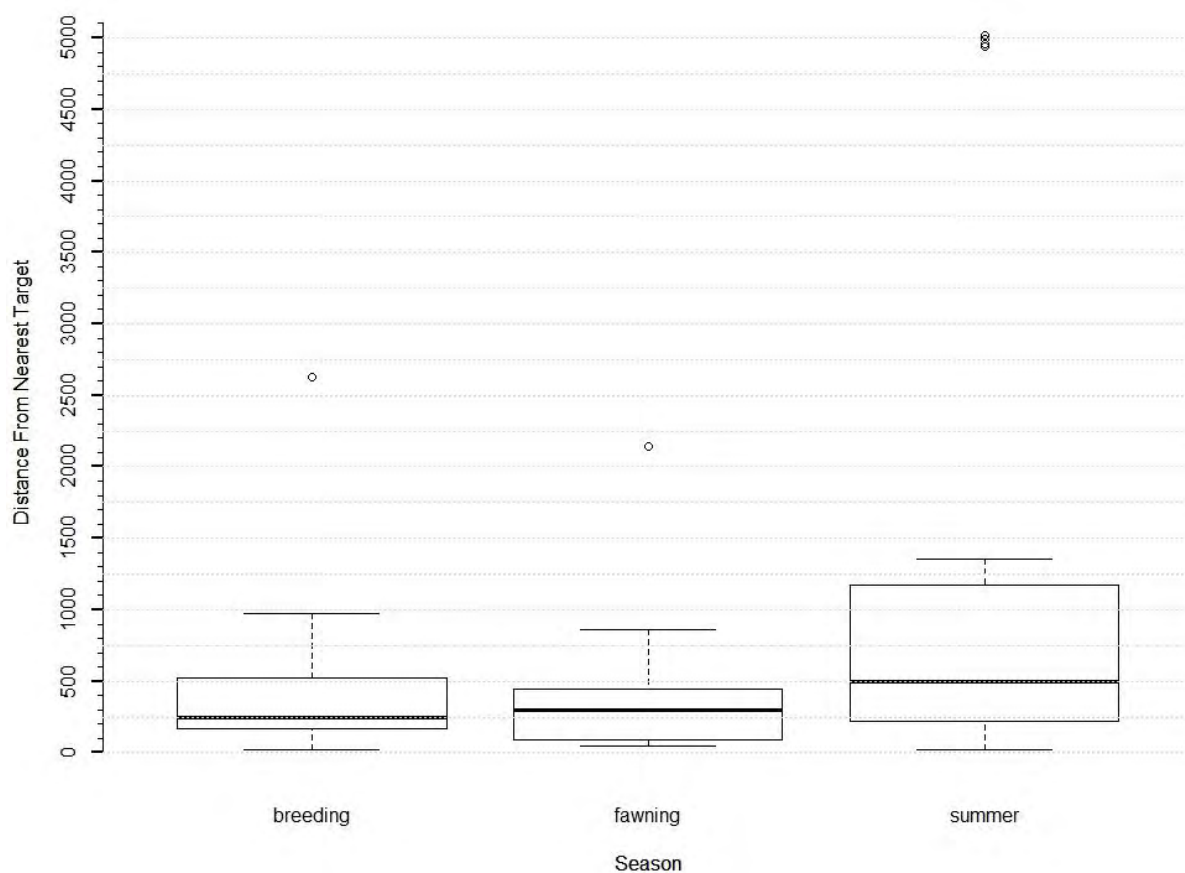


**Figure 13 Boxplot for Seasonal Variation in Hotspot Distance from Nearest Target**

These hotspot results and others, which are included in Appendix A, agree with a simple look at the number of sightings and hotspots within one kilometer of targets (Figure 14). Performing a quick buffer analysis shows that 58 percent of all sightings are within a one kilometer buffer. Based on these analyses, it confirms that SPH congregate near targets, though

the specific targets change throughout the year and between years. In general, the hotspots move more southward during the summer months each year, and move slightly northward during the winter months (Figure 15, Figure 16, Figure 17, Figure 18). Also, far fewer sightings are made throughout the range during the summer months. Results of each hotspot calculation for the last four years were produced as maps, and are included in Appendix A of this thesis.

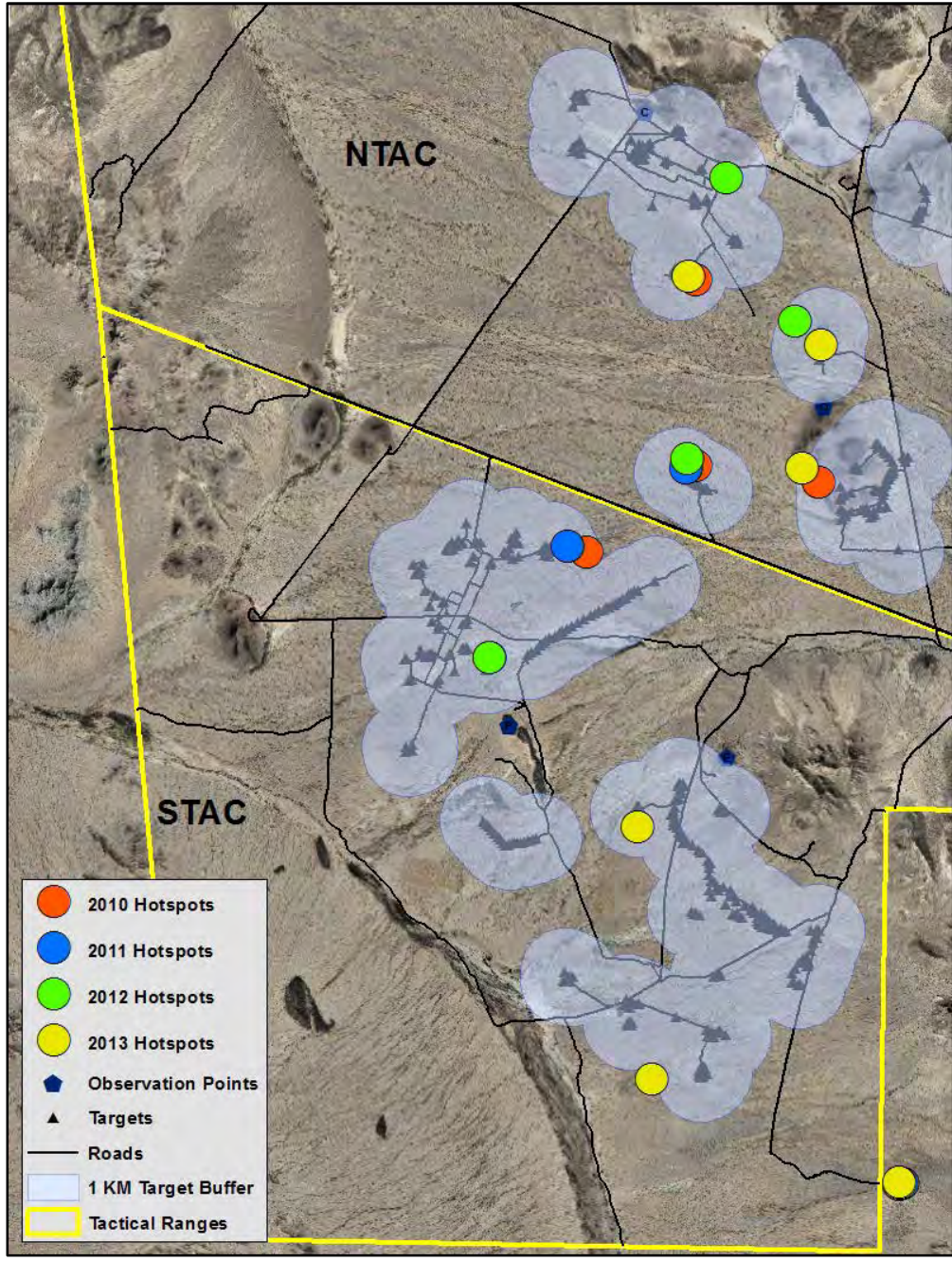


Figure 14 Annual Hotspots from 2010-2013 Above 1KM Target Buffer

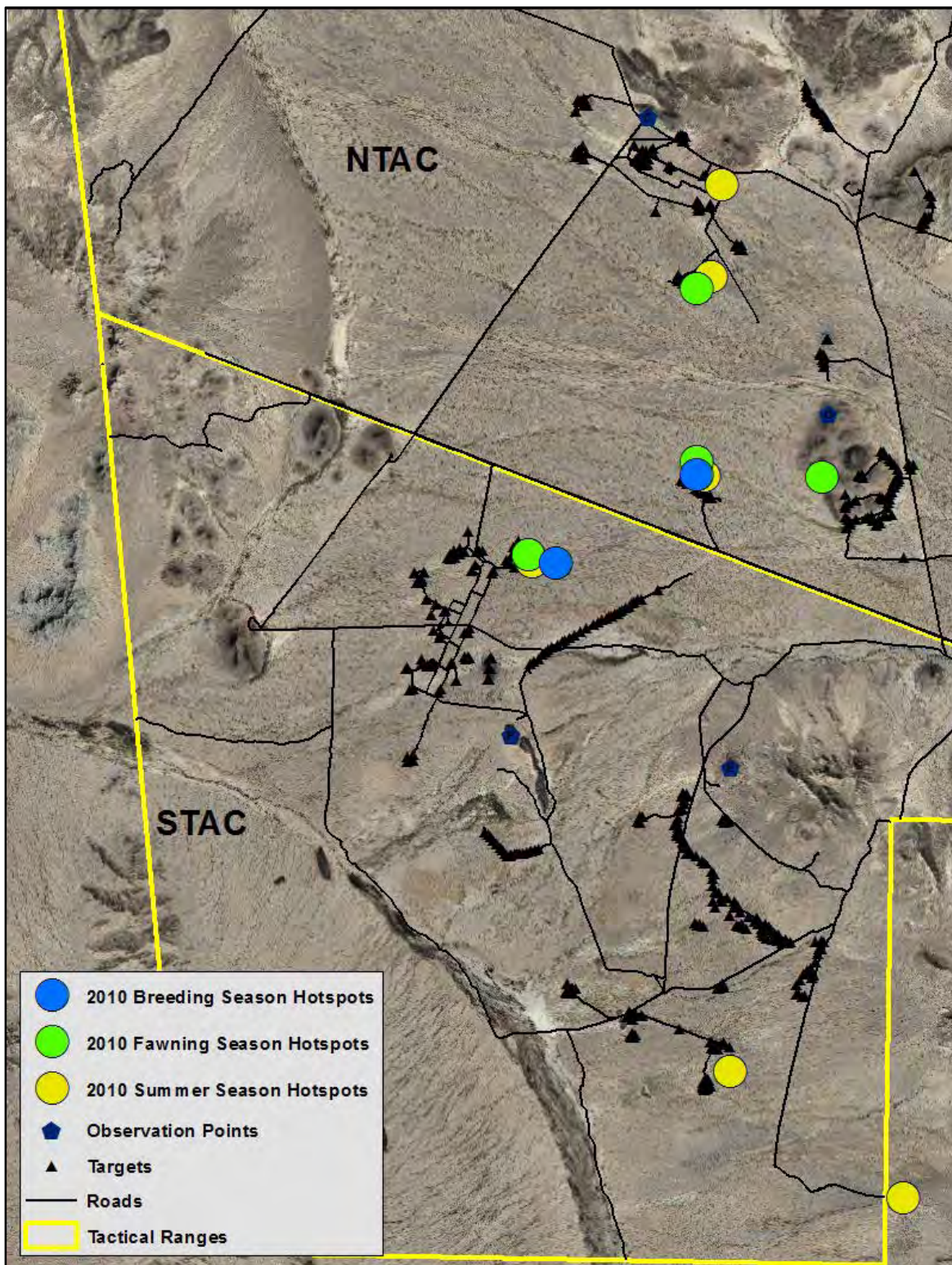


Figure 15 Seasonal Hotspots for 2010

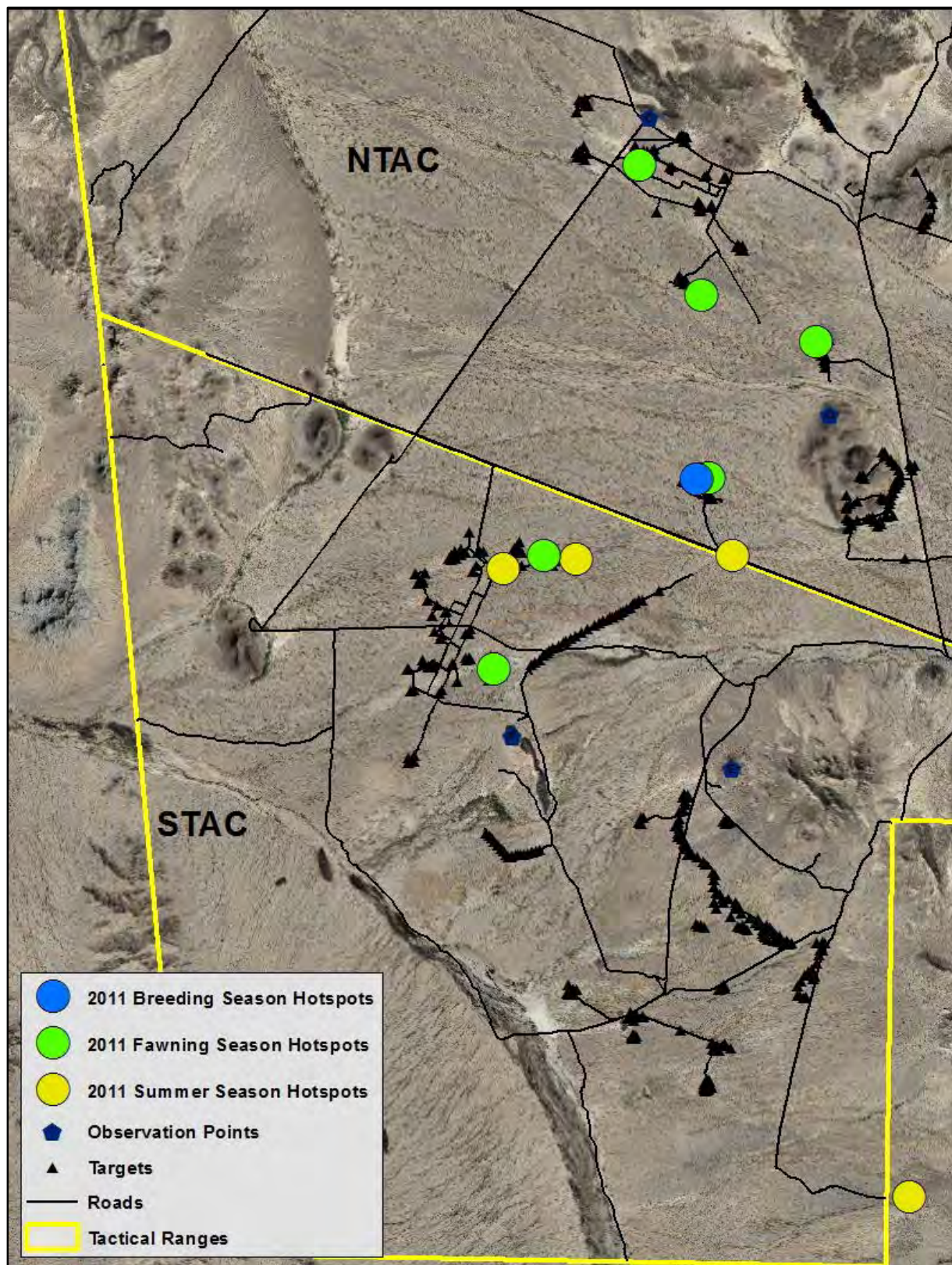


Figure 16 Seasonal Hotspots for 2011

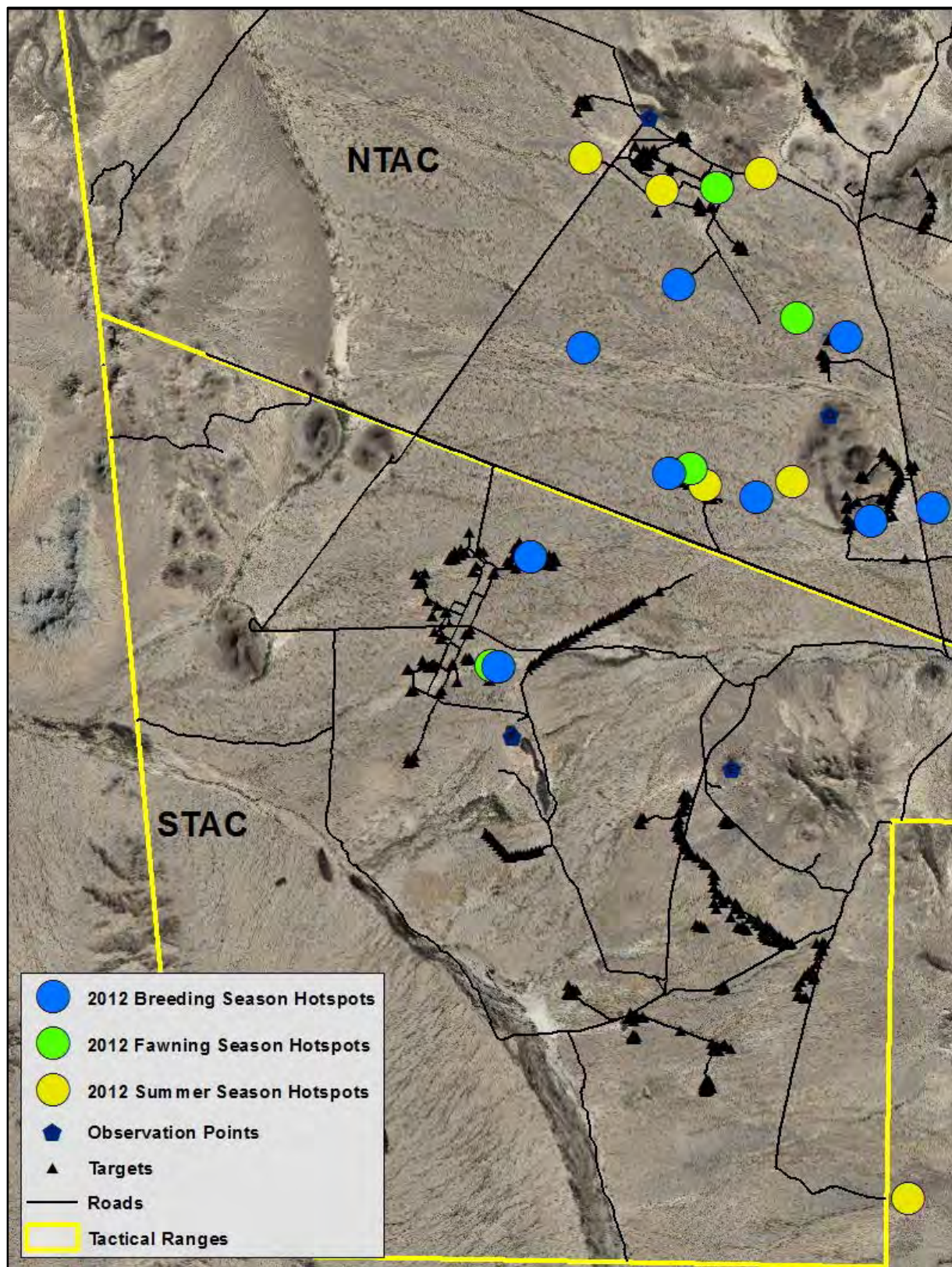


Figure 17 Seasonal Hotspots for 2012

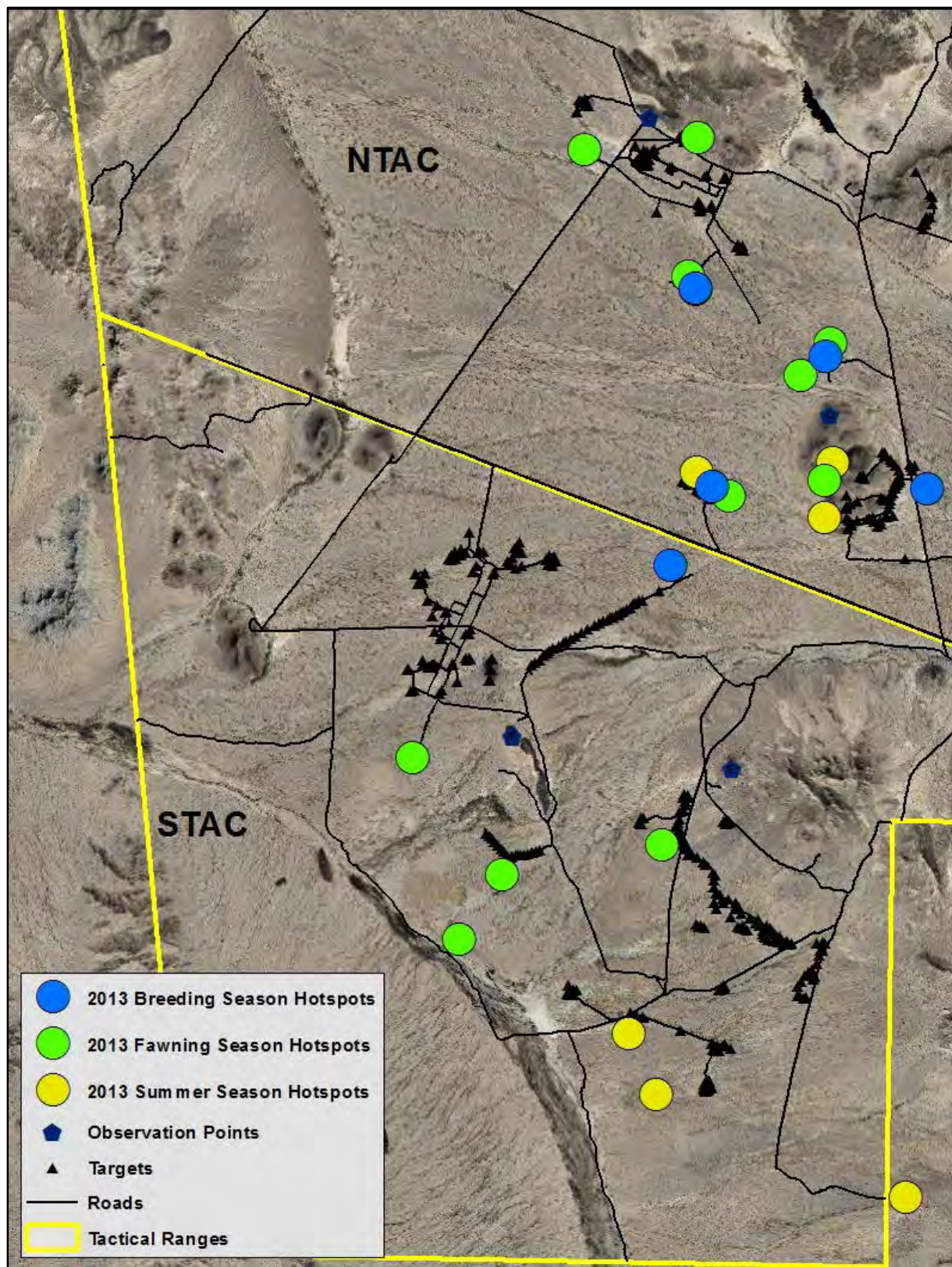


Figure 18 Seasonal Hotspots for 2013

## 4.2 Maximum Entropy Modelling

Results and model evaluation are based on the area under the curve (AUC), which represents model performance (Phillips, Anderson, and Schapire 2006). Separate models can then be compared to each other when evaluating which model to pursue further. Individual variables within a model run can be examined using the percent contribution, as calculated by the jackknife tests. Baldwin (2009) used an AUC evaluation scale where a value of less than 0.7 was considered uninformative, while values between 0.7 and 0.9 were considered good, and values greater than 0.9 were considered very good. Two models were run to examine the effect of including a wetness index within the model. The first model, including the wetness index, also included the target distance, road distance, observer distance, and slope. The second model removed the wetness index, but was otherwise the same.

The 1,000 replicates of the first model, which incorporated the wetness index, produced an average AUC of 0.803, with a standard deviation of 0.166 (Figure 19). When examining individual variable response curves, observer distance and road distance had a certain amount of variation present between replicates, while the remaining three variables had almost no variation between replicates (Figure 20). The jackknife test results for each variable on AUC values show that targets had the most impact as a standalone variable, as the model AUC went down significantly when it was removed from the model (Figure 21). The most important variable shown is the target distance, as it had the highest AUC value when it was the only variable considered, and the model AUC drops significantly when it was removed. The three variables above it (observer distance, road distance, and slope) had moderate AUC results if they were the only variable, but when removed from the overall model, there was little change. The wetness

index variable had very little impact on its own, and when removed, increased the model AUC, prompting the second model run, excluding the wetness index.

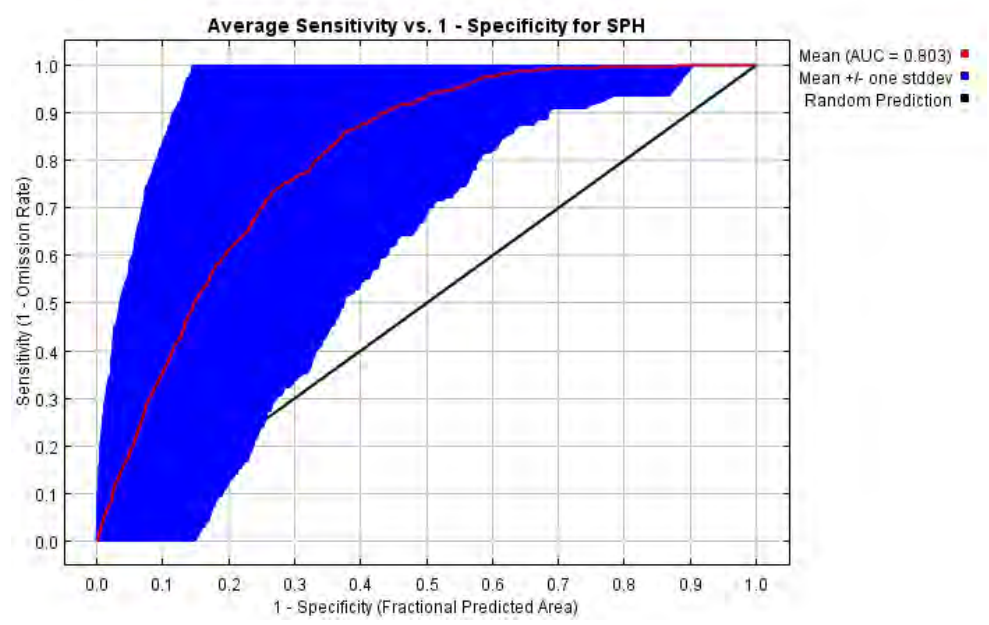


**Figure 19 Average AUC for 1,000 Replicates Including the Wetness Index**

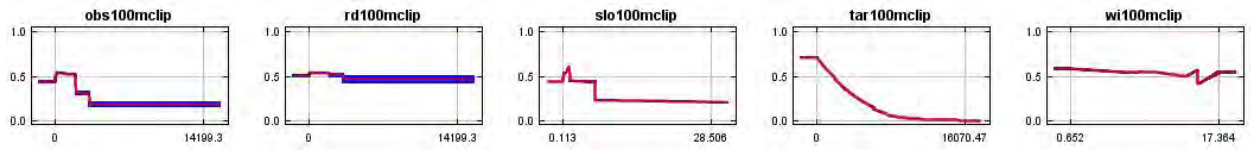


**Figure 20 Variable Response Curves for 1,000 Replicates Including the Wetness Index.**

**From Left to Right the Variables Shown Include Observer Distance, Distance from Road, Slope, Distance from Target, and Wetness Index**

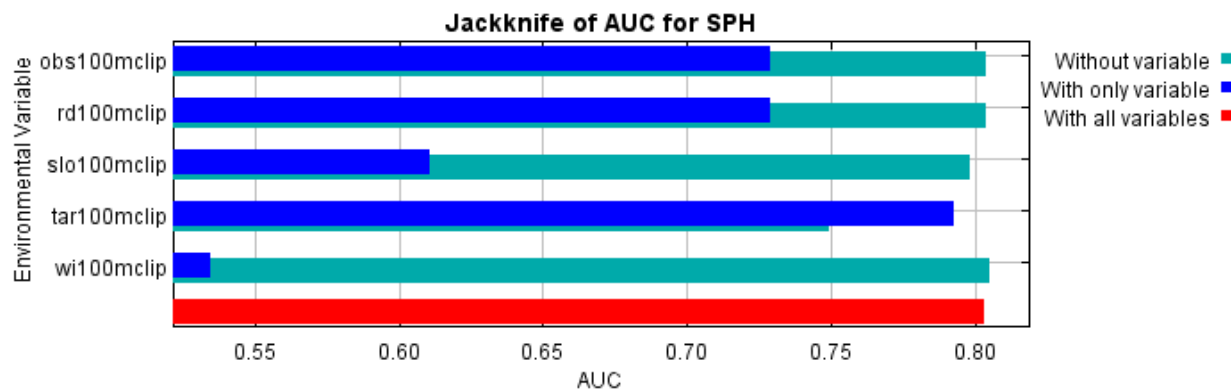


**Figure 21 Jackknife Test on AUCs for 1,000 Replicates Including the Wetness Index. From Top to Bottom, the Environmental Variables Include, Observer Distance, Distance from Roads, Slope, Distance from Targets, and Wetness Index**

The second model, excluding the wetness index variable, increased the average AUC value to 0.805 and lowered the standard deviation to 0.150 (Figure 22). The increase, though minimal, was an improvement. Variable response curves remained the same, as did the jackknife test results. Without the wetness index, the jackknife test is more obvious in showing that the target layer is most important. What is interesting is that while both observation distance and road distance perform better than slope when considered on their own, slope causes the next largest decrease in overall model AUC when it is removed (Figure 23).

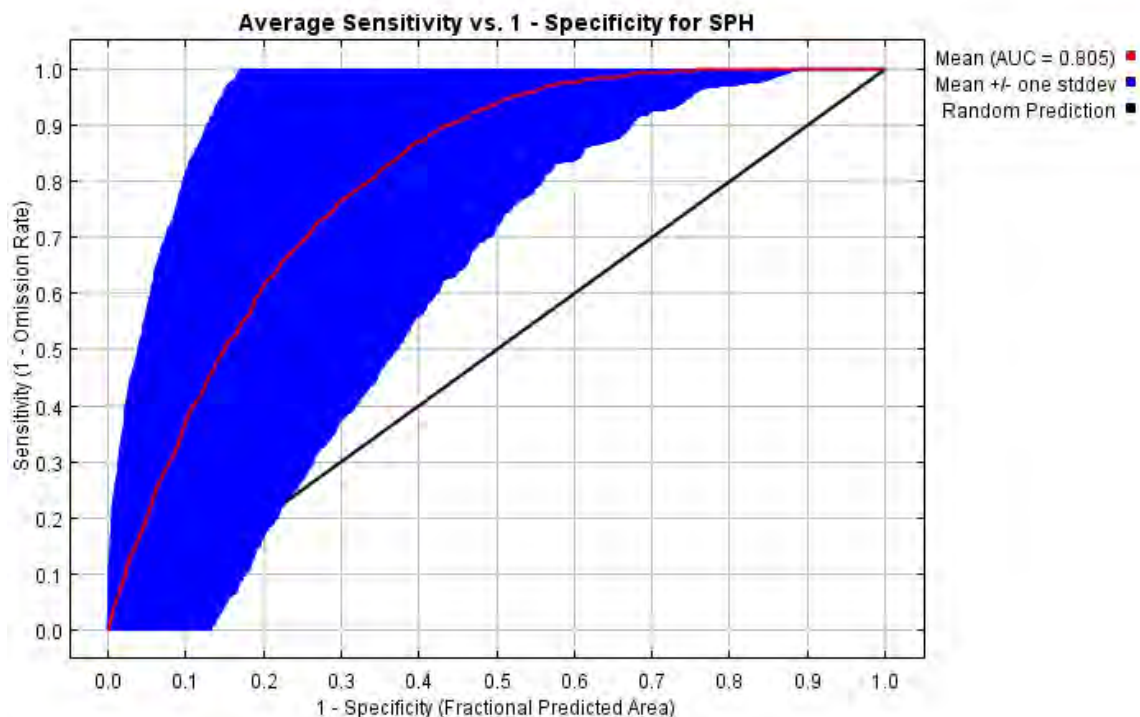


**Figure 22 Average AUC for 1,000 Replicates with the Wetness Index Removed**

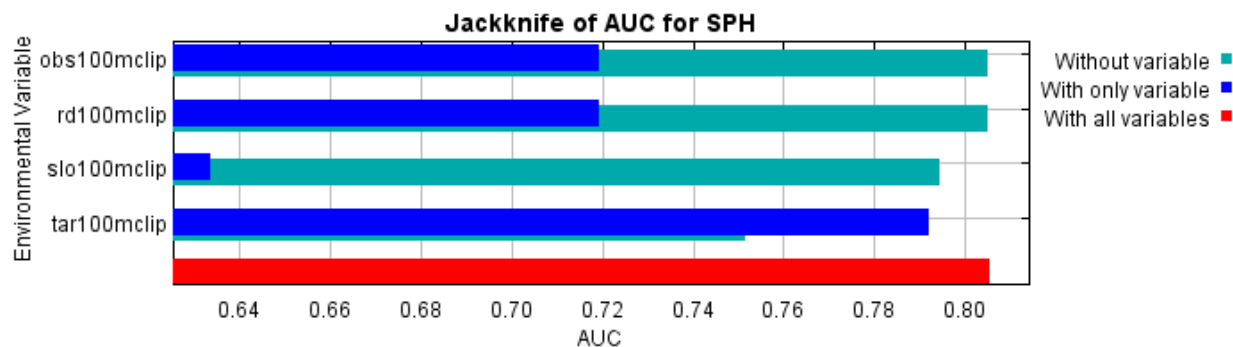


**Figure 23 Jackknife Test on AUCs for 1,000 Replicates with the Wetness Index Removed.**

**From Top to Bottom, the Environmental Variables Include Observer Distance, Distance from Roads, Slope, and Distance from Targets**

Comparing the percent contribution of variables from the two runs shows an increase for target distance and slope, but a decrease in observer distance (Table 3). Even though the percent contribution was higher for observer distance, it was the slope that had a larger effect on the

model performance. Importantly, no variable increased the overall model AUC when removed from the run.

**Table 3 Percent Contribution of Variables in the Two Model Runs**

<b>Variable</b>	<b>Percent contribution (With Wetness Index)</b>	<b>Percent contribution (NO Wetness Index)</b>
Target Distance	71.0	78.1
Observer Distance	22.2	10.8
Slope	5.2	7.9
Wetness Index	1.0	NA
Road Distance	0.5	3.1

Once the second model was identified as performing better, with a higher AUC value, the output raster probability layer was imported into ArcMap and examined (Figure 24). Each cell of the raster has a value related to the probability of detecting a SPH at its location. This raster was produced using all of the telemetry sightings for training, and the visual only sightings for testing. Seasonal or even monthly predictions could be made in order to more accurately predict locations for the future based on recent data only.

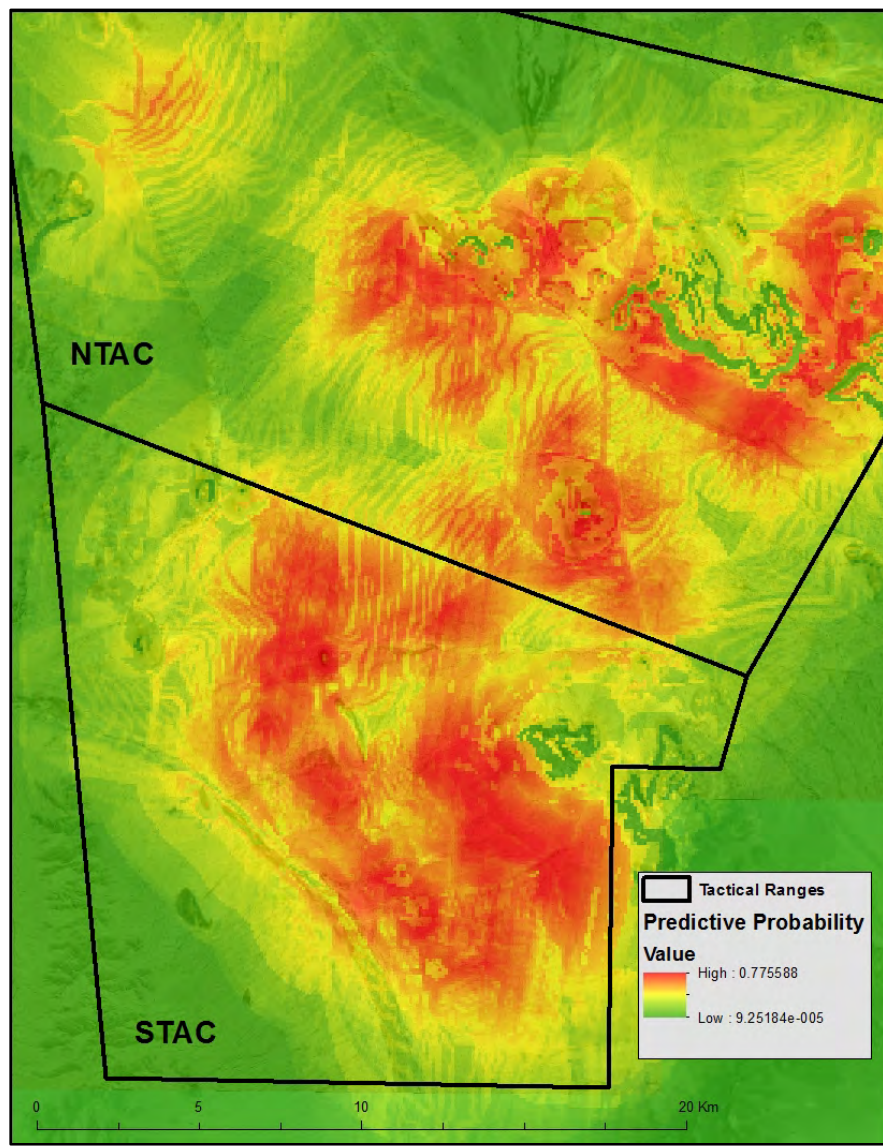


**Figure 24 Predictive Output Raster from the Second Model, Showing Probability of a Sighting**

The third model, using all the sighting data and the subsample method for calculating statistics produced a slightly lower AUC value of 0.791 (Figure 25). Where this model improved significantly was in the standard deviation, which came in at 0.004, as compared to the 0.166 and 0.150 of the first and second models. The response curves and jackknife tests were no different

from the first two models. The third model's output map shows a smoother distribution of high predictive values, though the overall predictive ability is lower (Figure 26).

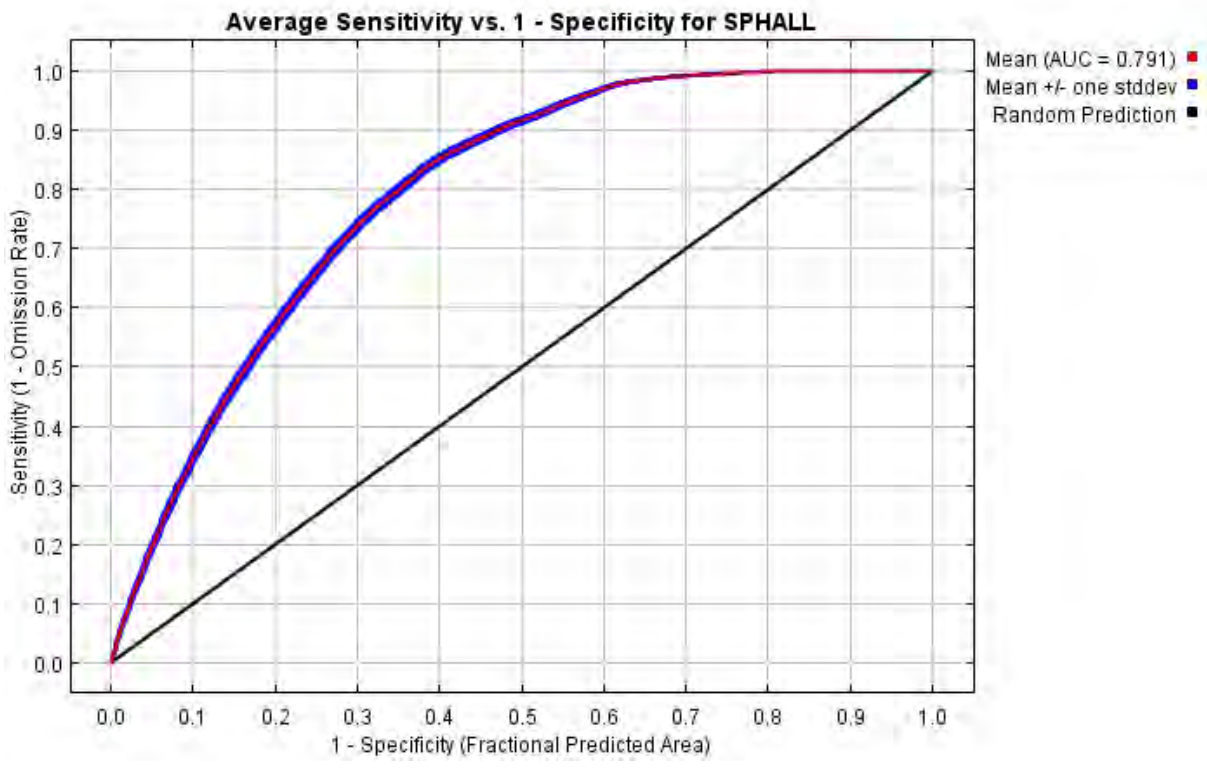


**Figure 25 Average AUC for 1,000 Replicates Using All Sightings with the 25 Percent Subsample Statistical Method**

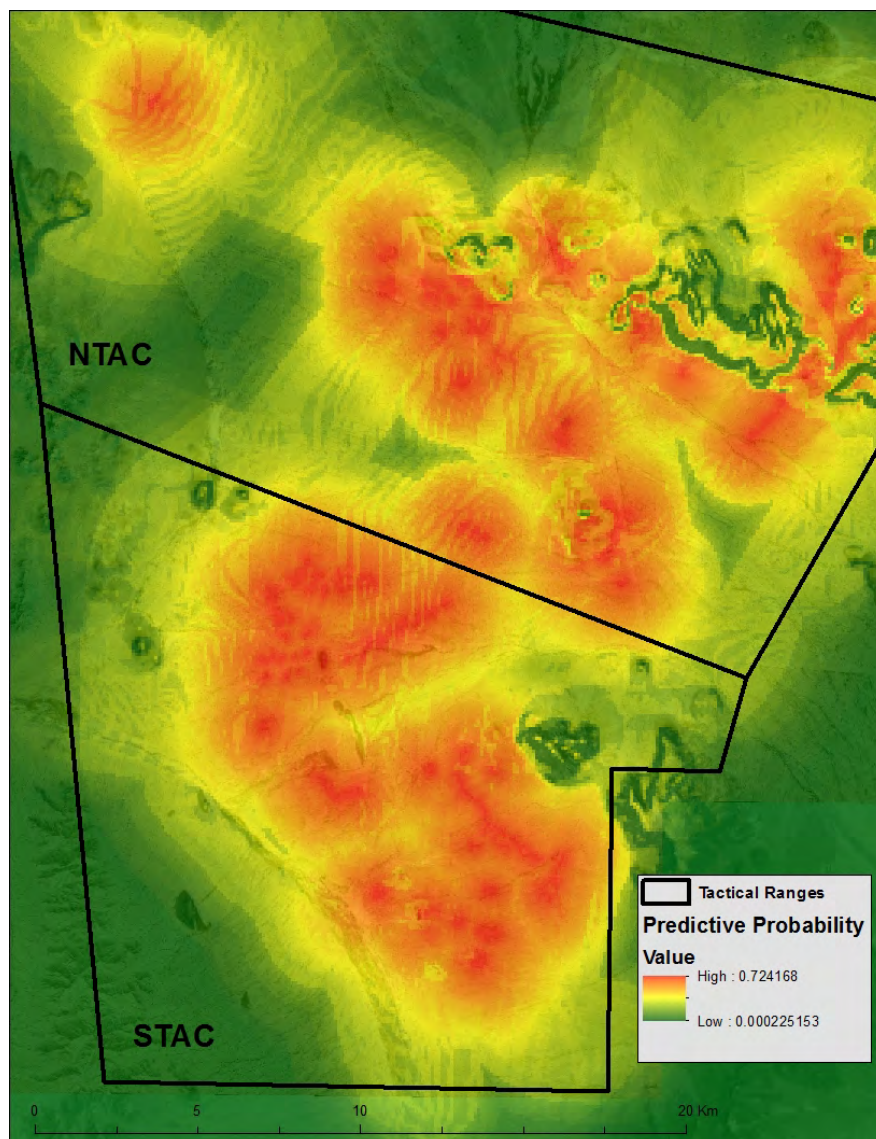


**Figure 26 Predictive Output Raster from the Third Model, Showing Probability of a Sighting**

Models four and five used telemetry only, then visual only data respectively for input locations, and the 25 percent subsample to calculate the AUC. Both AUC values were higher than for model two and model three, with standard deviations much lower than model two, and comparable to model three (Table 4). Though the overall AUC values were higher, the jackknife test and residuals remained the same when compared to the previous models.

**Table 4 Model Comparison of AUC and Standard Deviation Values**

	<u>Model 1</u>	<u>Model 2</u>	<u>Model 3</u>	<u>Model 4</u>	<u>Model 5</u>
	*	**	***	****	*****
<b>Variables</b>	5	4	4	4	4
Target Distance	x	x	x	x	x
Observer Distance	x	x	x	x	x
Slope	x	x	x	x	x
Road	x	x	x	x	x
Wetness Index	x	-	-	-	-
AUC Value	0.803	0.805	0.791	0.814	0.816
Standard Deviation	0.166	0.150	0.004	0.008	0.005

- \* All variables, telemetry for training, visual for testing
- \*\* No wetness index, telemetry for training, visual for testing
- \*\*\* No wetness index, all sightings, 75% training, 25% testing
- \*\*\*\* No wetness index, telemetry only sightings, 75% training, 25% testing
- \*\*\*\*\* No wetness index, visual only sightings, 75% training, 25% testing

## CHAPTER 5: CONCLUSION AND DISCUSSION

The results from this study confirm those from previous studies that used pre-2005 data, showing high densities of use, and high probabilities of future use, surrounding targets and disturbed areas (Krausman et al. 2005b). This thesis provides a demonstration of a different tool's ability to analyze and portray use of the target range by SPH. Unlike the study by Krausman et al. (2005b), it allows users to examine various environmental variables at any particular scale to decide which are most important when considering the future preference of SPH for a particular location.

Both the hotspot analysis and distribution model indicate that SPH have strong preference for areas at and around target structures. The few times a hotspot location was more than one kilometer from a target, it was located at an artificial water tank just east of the southeastern corner of target range. SPH used all of the range, but visual inspection makes apparent locations where more sightings occur (Figure 9). The majority of hotspots from 2010 to 2014 are located among four areas. These locations are more or less central within the range, including the northernmost targets on STAC and the southernmost targets on NTAC. The maps with more hotspot locations show that SPH were more spread out, and therefore there were more locations where the highest 20 percent density values occurred. Fewer hotspots show less spreading, and more clumping.

When the hotspots were examined on a seasonal time scale, the summer season stood out from the breeding and fawning seasons in that the distance from these hotspots to the nearest target was greater. This agrees with observations and sightings during the summer months, because many SPH move southwest towards the food and water station, while others leave the study area entirely. When the food station hotspots were removed from the analysis for each

season (they only occurred in the summer season of each year), the results of the ANOVA determined there was no significant difference in distance from targets between seasons. This emphasizes the effect of the food and water station on the SPH locations. During the breeding and fawning seasons, the SPH have the same access to that location as during the summer months, but choose to forage elsewhere. In this way, the food and water station provides a resource that has a significant impact on SPH location during the summer season of each year.

Before this study, the biologists monitoring the SPH had not identified the influence of roads on SPH sightings. Krausman et al. (2005b) examined roads and disturbance, though at a much coarser scale, by marking a one kilometer block as either having a road or a target or undisturbed. If there was a road anywhere within that block then it was given that attribute. Their study showed a high use of roads by SPH, with 70 percent of the road blocks having SPH sightings. These results show a high usage of road blocks by SPH, though I would argue that this method is not useful because roads are interspersed practically everywhere throughout the range, so it is difficult to get anywhere far from a road. Because of this, the one kilometer scale will inaccurately show roads as being important. By looking at the roads layer at a closer scale in this thesis, the effect of roads on SPH sightings is minimal, while the effect of targets remains high. There are times when SPH are seen walking along roads, traveling or foraging, though not often.

The results from the Maxent analysis show that the roads have very little effect on the pronghorn locations, in that when removed from the analysis, model performance did not decrease. Gavin and Komers (2006) examined the effects of various intensities of human disturbance on American pronghorn and found that while there did not appear to be any strong preference towards or away from roads, there was increased vigilance and less foraging time within groups near roads. The roads in this study consisted of public roads with average traffic

values estimated by the department of transportation between <10 to >300 vehicles per day. They also noticed that larger groups were affected less in this way than individuals or small groups. Observation distance had the same result within the model's jackknife tests, though when considering the percent contribution to the model, it takes a much larger percentage than the road distance or the other variables. This is interesting because when examining the jackknife test, they are almost exactly the same in AUC model performance values. Prior studies always mention potential bias caused by observation locations (Krausman et al. (2005b), though none look at observation distance or type of sighting as a way to mediate this bias.

Interestingly, slope appears to have the most negative effect on the model AUC when removed, after target distance. Unfortunately, because most of the study area is relatively flat, this is hard to corroborate through observation in the field. It is true that the SPH are rarely on the hills themselves, but they are sometimes seen in between hills, where access is limited to being on the hill's steep slope at some point while traveling.

The third model results showed that while the predictive ability decreased slightly, the variance present decreased greatly. This shows that there are differences between the telemetry locations and the visual locations. SPH are seen more easily close to observers. The third model included all sightings, which means that there were many groups that were not specified as having been seen first, or whether their sighting was due to a telemetry animal being within the group. The fact that a random 25 percent of the sightings were chosen to test with, I believe, explains the lower AUC value because it is unknown which locations were used for training or testing. Models four and five had higher AUC values and lower standard deviations because each 25 percent test dataset was taken from the same dataset as the 75 percent used in training the algorithm. This is what I expected, and why I don't think they are the best option for the primary

model. Observer bias is an issue, in this study and others, and should be taken into account. That the models using only one type of sighting performed better, with less variation in runs, supports the idea that the two sightings are different enough from each other to affect the model's performance. I believe that by using telemetry only sightings for training, and visual sightings for testing, a portion of observer bias is accounted for, even though the model AUC is lower and the standard variation is larger.

Future analyses of this type should explore the use of precipitation interpolation layers, as well as detailed vegetation classifications for supplemental environmental variables. Because the study area is small relative to the scale at which these variables are currently available, they were not included in the analysis. The addition of a bias layer could potentially help as well, these methods attempted to account for visibility bias by using telemetry only sightings for training and visual only for testing. As observation points are positioned to provide maximum visibility to targets, this is definitely an important consideration when interpreting the results. Vegetation types also have different cover values, as small trees are harder to see through than short grass or shrubs. Perhaps a layer built from the vegetation type could represent an index of visibility within the model.

Other than the addition of new variables into the model, the time scale being analyzed will definitely affect the predictive capacity of the output. If the SPH biologists and monitors are interested in a prediction of sighting locations for the next month, the analysis should be run using recent sightings only, to provide the level of variation required.

## REFERENCES

- Anderson, Tessa K. 2009. "Kernel Density Estimation and K-means Clustering to Profile Road Accident Hotspots." *Accident Analysis and Prevention* 41: 359-364.
- Baldwin, Roger A. 2009. "Use of Maximum Entropy Modeling in Wildlife Research." *Entropy* 11: 854-866.
- Beyer, H. L. 2012. *Geospatial Modelling Environment* (Version 0.7.2.1). URL <http://www.spatalecology.com/gme>.
- Blundell, Gail M., Julie A. K. Maier, and Edward M. Debevec. 2001. "Linear Home Ranges: Effects of Smoothing, Sample Size, and Autocorrelation on Kernel Estimates." *Ecological Monographs* 71: 469-489.
- Bright, Jill L. and John J. Hervert. 2005. "Adult and Fawn Mortality of Sonoran Pronghorn." *Wildlife Society Bulletin* 33: 43-50.
- deVos, James C. and William H. Miller. 2005. "Habitat Use and Survival of Sonoran Pronghorn in Years with Above-average Rainfall." *Wildlife Society Bulletin* 33: 35-42.
- Downs, Joni A. 2010. "Time-geographic Density Estimation for Moving Point Objects." *Geographic Information Science* 6292: 16-26.
- Downs, Joni A. and Mark W. Horner. 2008. "Effects of Point Pattern Shape on Home-range Estimates." *Journal of Wildlife Management* 72: 1813-1818.
- Elith, Jane, Steven J. Phillips, Trevor Hastie, Miroslav Dudik, Yung E. Chee, and Colin J. Yates. 2011. "A Statistical Explanation of MaxEnt for Ecologists." *Diversity and Distributions* 14: 43-57.
- Er, A. C., M. H. Rosli, A. Asmahani, M. R. Mohamad Naim, and M. Harsuzilawati. 2010. "Spatial Mapping of Dengue Incidence: A Case Study in Hulu Langat District, Selangor,

- Malaysia.” *International Journal of Environmental, Ecological, Geological and Mining Engineering* 4: 25-29.
- ESRI. 2012. ArcGIS Desktop: Release 10.1. Redlands, CA: Environmental Systems Research Institute.
- Fox, L. M. “Nutritional content of forage in Sonoran pronghorn habitat, Arizona.” MS Thesis, University of Arizona, Tucson, 1997.
- Gavin, Shannon D. and P. E. Komers. 2006. “Do Pronghorn (*Antilocapra americana*) Percieve Roads as a Predation Risk?” *Canadian Journal of Zoology* 84: 1775-1780.
- Gu, Weidong and Robert K. Swihart. 2004. “Absent or Undetected? Effects of Non-detection of Species Occurrence on Wildlife-habitat Models.” *Biological Conservation* 116: 195-203.
- Hernandez, Pilar A., Catherine H. Graham, Lawrence L. Master, and Deborah L. Albert. 2006. “The Effect of Sample Size and Species Characteristics on Performance of Different Species Distribution Modeling Methods.” *Ecography* 29: 773-785.
- Hervert, John J., Jill L. Bright, Robert S. Henry, Linden A. Piest, and Mark T. Brown. 2005. “Home-range and Habitat-use Patterns of Sonoran Pronghorn in Arizona.” *Wildlife Society Bulletin* 33: 8-15.
- Hervert, John J., Linden A. Piest, W. Ballard, R. S. Henry, Mark T. Brown, and S. Boe. 1997. “Sonoran Pronghorn Population Monitoring: Progress Report.” Arizona Game and Fish Department, Technical Report, 126. Phoenix, AZ.
- Hosack, Dennis A., P. S. Miller, John J. Hervert, and R. C. Lacy. 2002. “A Population Viability Analysis for the Endangered Sonoran Pronghorn, *Antilocapra americana sonoriensis*.” *Mammalia* 66: 207-229.

- Kie, John G., Jason Matthiopoulos, John Fieberg, Roger A. Powell, Francesca Cagnacci, Michael S. Mitchell, Jean-Michel Gaillard, and Paul R. Moorcroft. 2010. "The Home-range Concept: are Traditional Estimators Still Relevant with Modern Telemetry Technology?" *Philosophical Transactions of the Royal Society B* 365: 2221-2231.
- Krausman, Paul R., John R. Morgart, Lisa K. Harris, Chantal S. O'Brien, James W. Cain III, and Steven S. Rosenstock. 2005. "Introduction: Management for the Survival of Sonoran Pronghorn in the United States." *Wildlife Society Bulletin* 33: 5-7.
- Krausman, Paul R., Lisa K. Harris, Sarah K. Haas, Kiana K. G. Koenen, Pat Devers, Daniel Bunting, and Mark Barb. 2005. "Sonoran Pronghorn Habitat Use on Landscapes Disturbed by Military Activities." *Wildlife Society Bulletin* 33: 16-23.
- Krausman, Paul R., Lisa K. Harris, and Jon Francine. 2001. "Noise Effects of Military Overflights on Sonoran Pronghorn: Final Report." The University of Arizona, Tucson, AZ.
- Krausman, Paul R., John R. Morgart, Lisa K. Harris, Chantal S. O'Brien, James W. Cain, III, Steven S. Rosenstock. 2005. "Sonoran Pronghorn Literature: an Annotated Bibliography." *USGS Open-File Report* 2005-1265. U.S. Geological Survey, Southwest Biological Science Center, Sonoran Desert Research Station, The University of Arizona, Tucson, AZ.
- Krisp, Jukka M. and Stefan Peters. 2011. "Directed Kernel Density Estimation (DKDE) for Time Series Visualization." *Annals of GIS* 17: 155-162.
- Kumar, Sunil and Thomas J. Stohlgren. 2009. "Maxent Modeling for Predicting Suitable Habitat for Threatened and Endangered Tree *Canacomyrica monticola* in New Caledonia." *Journal of Ecology and Natural Environment* 1: 94-98.

- Lin, Yu-Pin, Hone-Jay Chu, Chen-Fa Wu, Tsun-Kuo Chang, and ChiuYang Chen. 2011. "Hotspot Analysis of Spatial Environmental Pollutants Using Kernel Density Estimation and Geostatistical Techniques." *International Journal of Environmental Research and Public Health* 8: 75-88.
- Liu, Hua and Donald E. Brown. 2003. "Criminal Incident Prediction Using a Point-pattern-based Density Model." *International Journal of Forecasting* 19: 603-622.
- Merow, Cory, Matthew J. Smith, and John A. Silander, Jr. 2013. "A Practical Guide to MaxEnt for Modeling Species' Distributions: What it Does, and Why Inputs and Settings Matter." *Ecography* 36: 1058-1069.
- Mola-Yudego, Blas and David Gritten. 2010. "Determining Forest Conflict Hotspots According to Academic and Environmental Groups." *Forest Policy and Economics* 12: 575-580.
- Moreno, Roberto, Ricardo Zamora, Juan R. Molina, Angelica Vasquez, and Miguel A. Herrera. 2011. "Predictive Modeling of Microhabitats for Endemic Birds in South Chilean Temperate Forests Using Maximum Entropy (Maxent)." *Ecological Informatics* 6: 364-370.
- Morgart, John R., John J. Hervert, Paul R. Krausman, Jill L. Bright, and Robert S. Henry. 2005. "Sonoran Pronghorn Use of Anthropogenic and Natural Water Sources." *Wildlife Society Bulletin* 33: 51-60.
- Motsinger, J. 2013. Defenders of Wildlife Blog. "Road to Recovery: Sonoran Pronghorn." <http://www.defendersblog.org/2013/07/road-to-recovery-sonoran-pronghorn> (accessed 9 July 2014).
- Nelson, Trisalyn A. and Barry Boots. 2008. "Detecting Spatial Hot Spots in Landscape Ecology." *Ecography* 35: 556-566.

Ochenfels, R. Pronghorn antelope. Arizona Antelope Foundation.

[http://azantelope.org/Facts\\_Research/About\\_Pronghorn/about\\_pronghorn.html](http://azantelope.org/Facts_Research/About_Pronghorn/about_pronghorn.html)

(accessed 10 July 2014).

O’Gara, Bart W. 1978. “*Antilocapra americana*.” *Mammalian Species* 90: 1-7.

Phillips, Steven. 2005. "A Brief Tutorial on Maxent." *ATandT Research*.

Phillips, Steven J. and Miroslav Dudik. 2008. “Modeling of Species Distributions with Maxent: New Extensions and a Comprehensive Evaluation.” *Ecography* 31:161-175.

Phillips, Steven J., Miroslav Dudik, and Robert E. Schapire. “A Maximum Entropy Approach to Species Distribution Modeling.” In *Proceedings of the 21st International Conference on Machine Learning*, 655-662. ACM Press, New York, 2004.

Phillips, Steven J., Robert P. Anderson, and Robert E. Schapire. 2006. “Maximum Entropy Modeling of Species Geographic Distributions.” *Ecological Modelling* 190: 231-259.

Pronghorn Biologists. *Sonoran Pronghorn Monitoring Protocol*. Gila Bend and Barry M. Goldwater Range Complex, Gila Bend, AZ, 2012.

R Development Core Team. 2011. *R: A language and environment for statistical computing* (Version 3.1.0). R Foundation for Statistical Computing, Vienna, Austria. URL <http://www.R-project.org/>.

Ramp, Daniel, Joanne Caldwell, Kathryn A. Edwards, David Warton, and David B. Croft. 2005. “Modelling of Wildlife Fatality Hotspots Along the Snowy Mountain Highway in New South Wales, Australia.” *Biological Conservation* 126: 474-490.

Reid, F. A. *A field guide to mammals of North America*, 500-501. New York, NY: Houghton Mifflin Company, 2006.

- Seaman, D. Erran, Joshua J. Millspaugh, Brian J. Kernohan, Gary C. Brundige, Kenneth J. Raedeke, and Robert A. Gitzen. 1999. "Effects of Sample Size on Kernel Home Range Estimates." *Journal of Wildlife Management* 63: 739-747.
- Seaman D. Erran and Roger A. Powell. 2005. "An Evaluation of the Accuracy of Kernel Density Estimators for Home Range Analysis." *Ecology* 77: 2075-2075.
- Silverman, Bernard W. *Density Estimation for Statistics and Data Analysis*. London, UK: Chapman and Hall, 1986.
- Stephen, Catherine L., James C. Devos, Jr., Thomas E. Lee, Jr., John W. Bickham, James R. Heffelfinger, and Olin E. Rhodes Jr. 2005. "Population Genetic Analysis of Sonoran Pronghorn (*Antilocapra americana sonoriensis*)." *Journal of Mammalogy* 86: 782-792.
- Suarez-Seoane, Susana, Eladio L. Garcia de la Morena, Manuel B. Morales Prieto, Patrick E. Osborne, and Eduardo de Juana. 2008. "Maximum Entropy Niche-based Modelling of Seasonal Changes in Little Bustard (*Tetrax tetrax*) Distribution." *Ecological Modelling* 219: 17-29.
- Tetra Tech, Inc. *Ecological Factors that may Influence Sonoran Pronghorn: North and South Tactical Ranges, Barry M. Goldwater Range, Luke AFB, Arizona*. By Tetra Tech, Inc. San Bernardino, CA, 2005.
- Tinker, B. *Mexican Wilderness and Wildlife*. University of Texas Press, Austin, USA, 1978.
- United States Fish and Wildlife Service. *Final Revised Sonoran Pronghorn Recovery Plan*. Albuquerque, NM, 1998.
- United States Fish and Wildlife Service. *Fact Sheet: Sonoran Pronghorn*. Albuquerque, NM, 2003.

- United States Fish and Wildlife Service. *Final Environmental Assessment for Reestablishment of Sonoran Pronghorn*. Albuquerque, NM, 2010.
- Vander Wal, Eric and A. R. Rodgers. 2012. "An Individual-based Quantitative Approach for Delineating Core Areas of Animal Space Use." *Ecological Modelling* 224: 48-53.
- Wand, M. P. and M. C. Jones. *Kernel Smoothing*. London, UK: Chapman and Hall, 1995.
- Worton, B. J. 1989. "Kernel Methods for Estimating the Utilization Distribution in Home-range Studies." *Ecology* 70: 164-168.
- Xie, Zhixiao and Jun Yan. 2008. "Kernel Density Estimation of Traffic Accidents in a Network Space." *Computers, Environment and Urban Systems* 32:396-406.
- Yoakum, J. D. "Pronghorn." In *Big game of North America: ecology and management*, edited by J. L. Schmidt and D. L. Gilbert, 103-121. Washington, D.C.: Wildlife Management Institute and Harrisburg, PA: Stackpole Books, 1978.
- Yost, Andrew C., Steven L. Petersen, Michael Gregg, and Richard Miller. 2008. "Predictive Modeling and Mapping Sage Grouse (*Centrocercus urophasianus*) Nesting Habitat Using Maximum Entropy and a Long-term Dataset from Southern Oregon." *Ecological Informatics* 3: 375-386.

## APPENDIX A: HOTSPOT MAPS

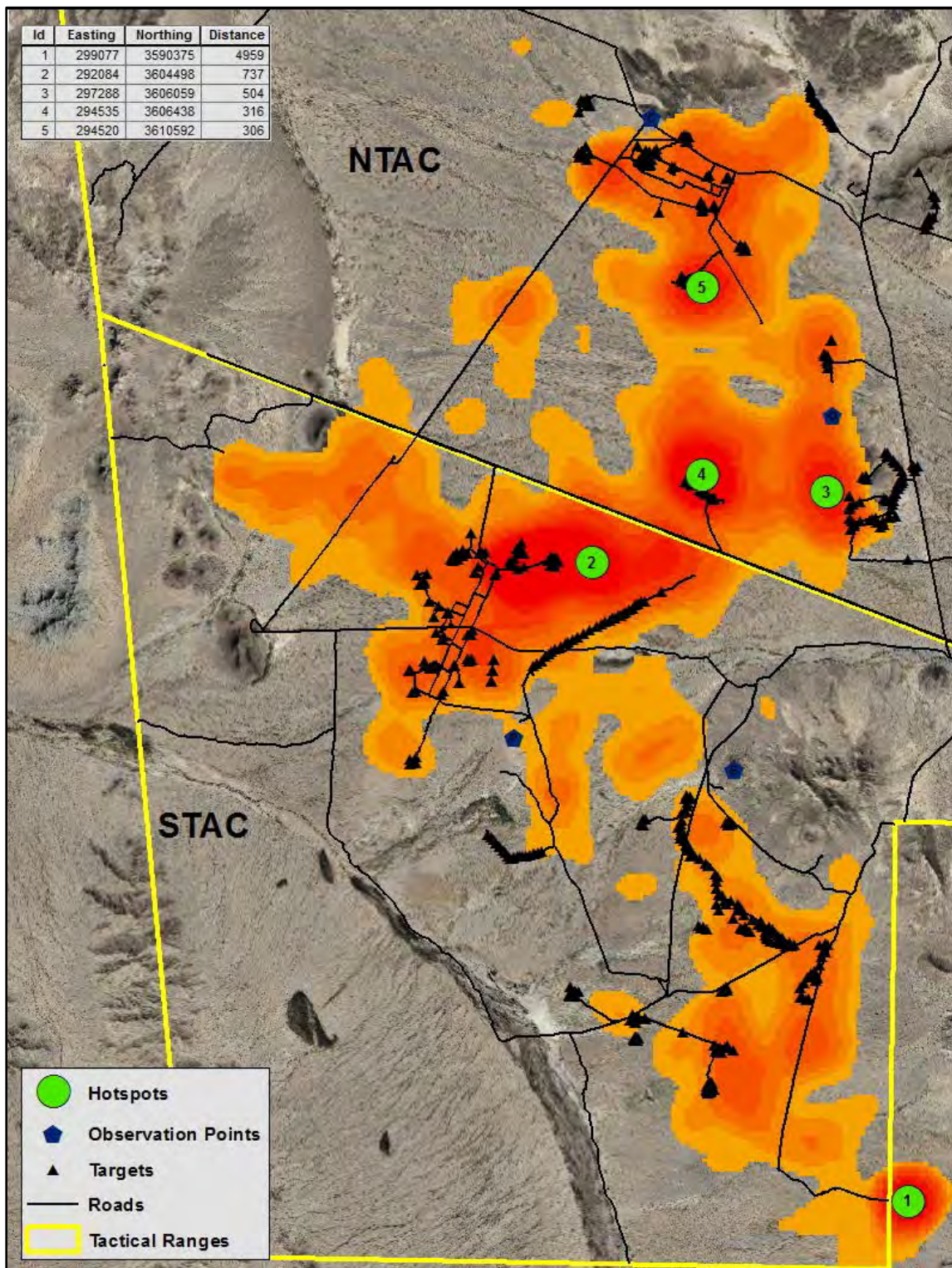


Figure 27 SPH 2010 Hotspot Map with Underlying KDE Raster

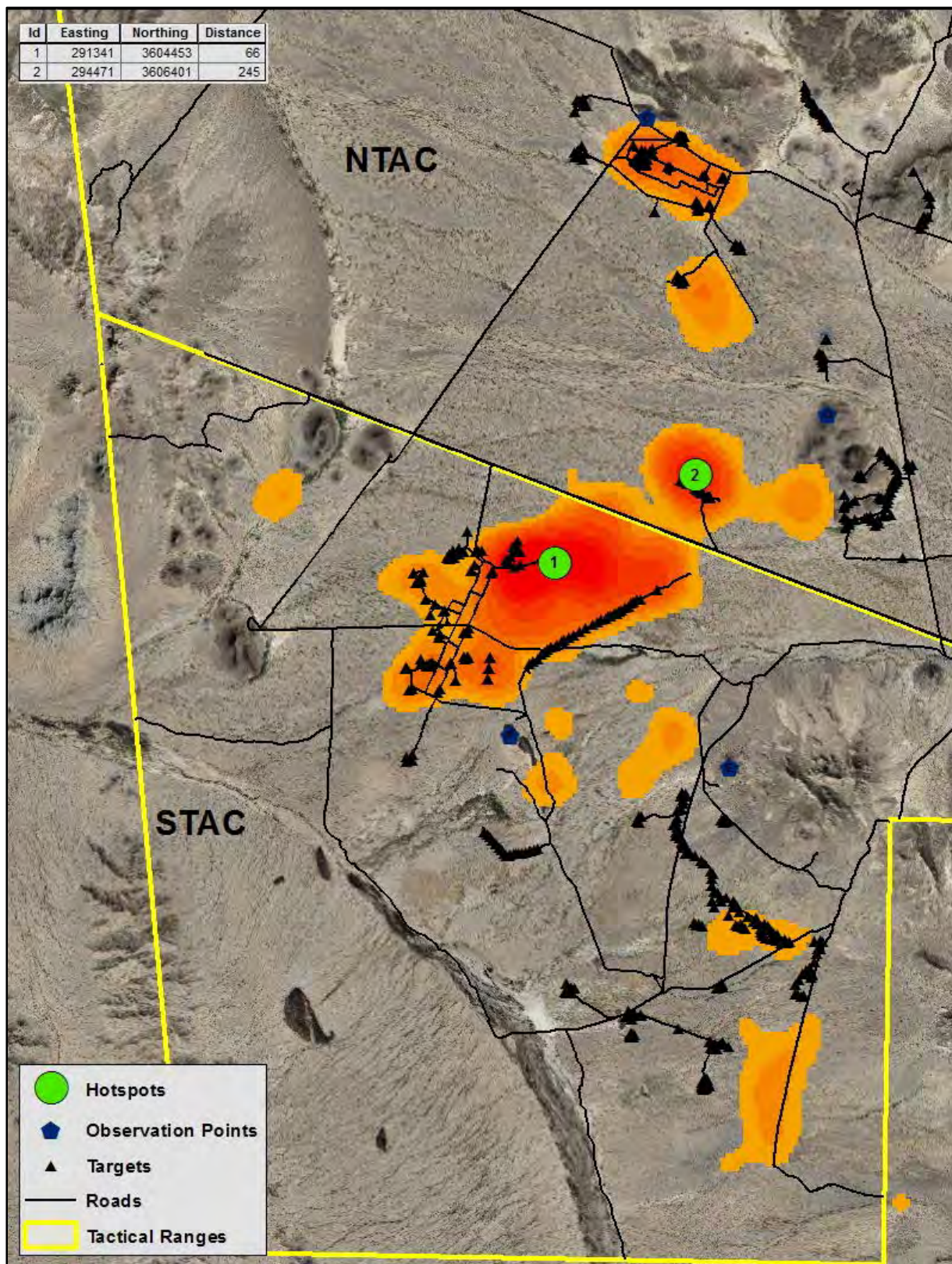


Figure 28 SPH 2010 Breeding Season Hotspot Map with Underlying KDE Raster

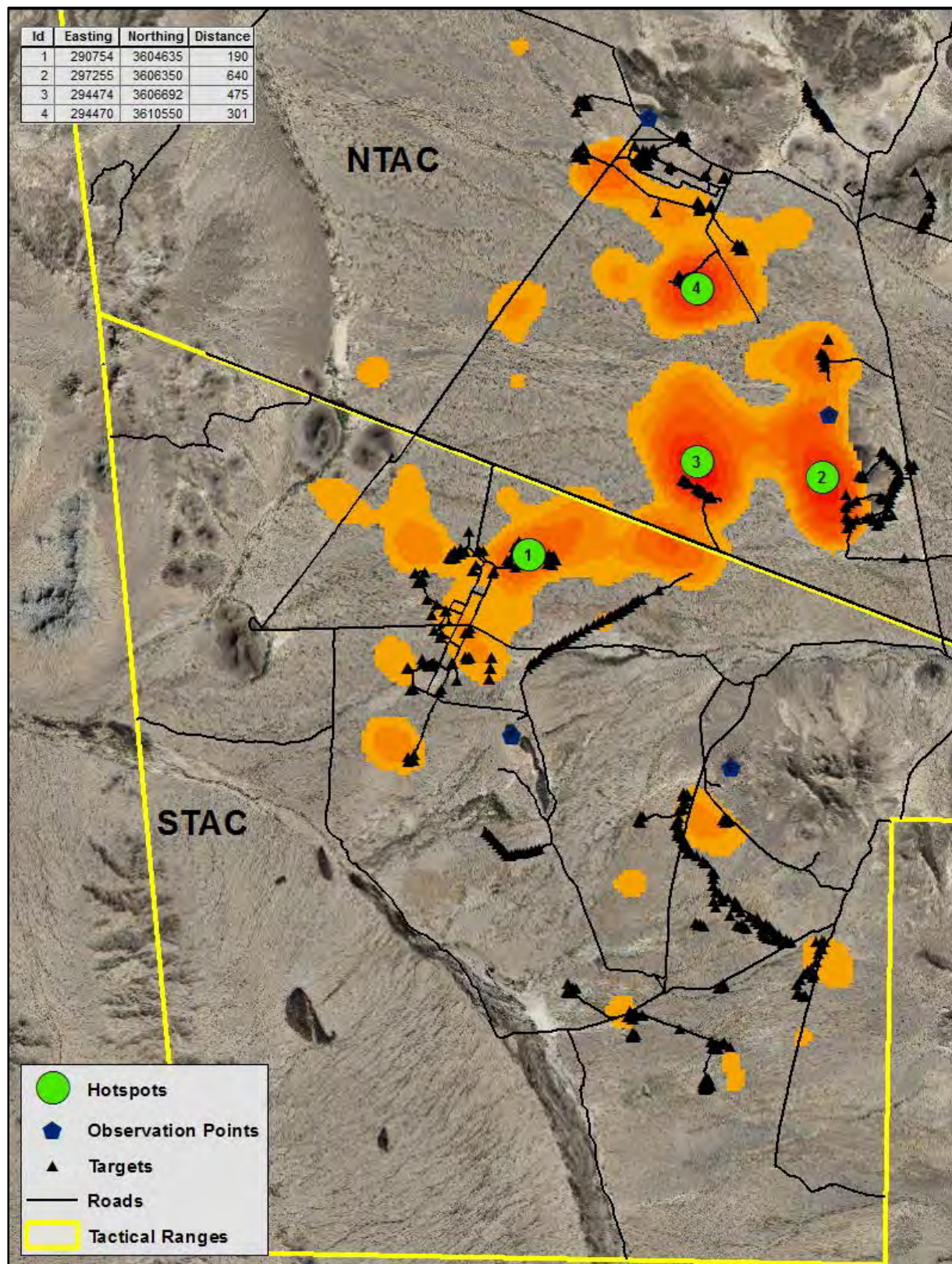


Figure 29 SPH 2010 Fawning Season Hotspot Map with Underlying KDE Raster

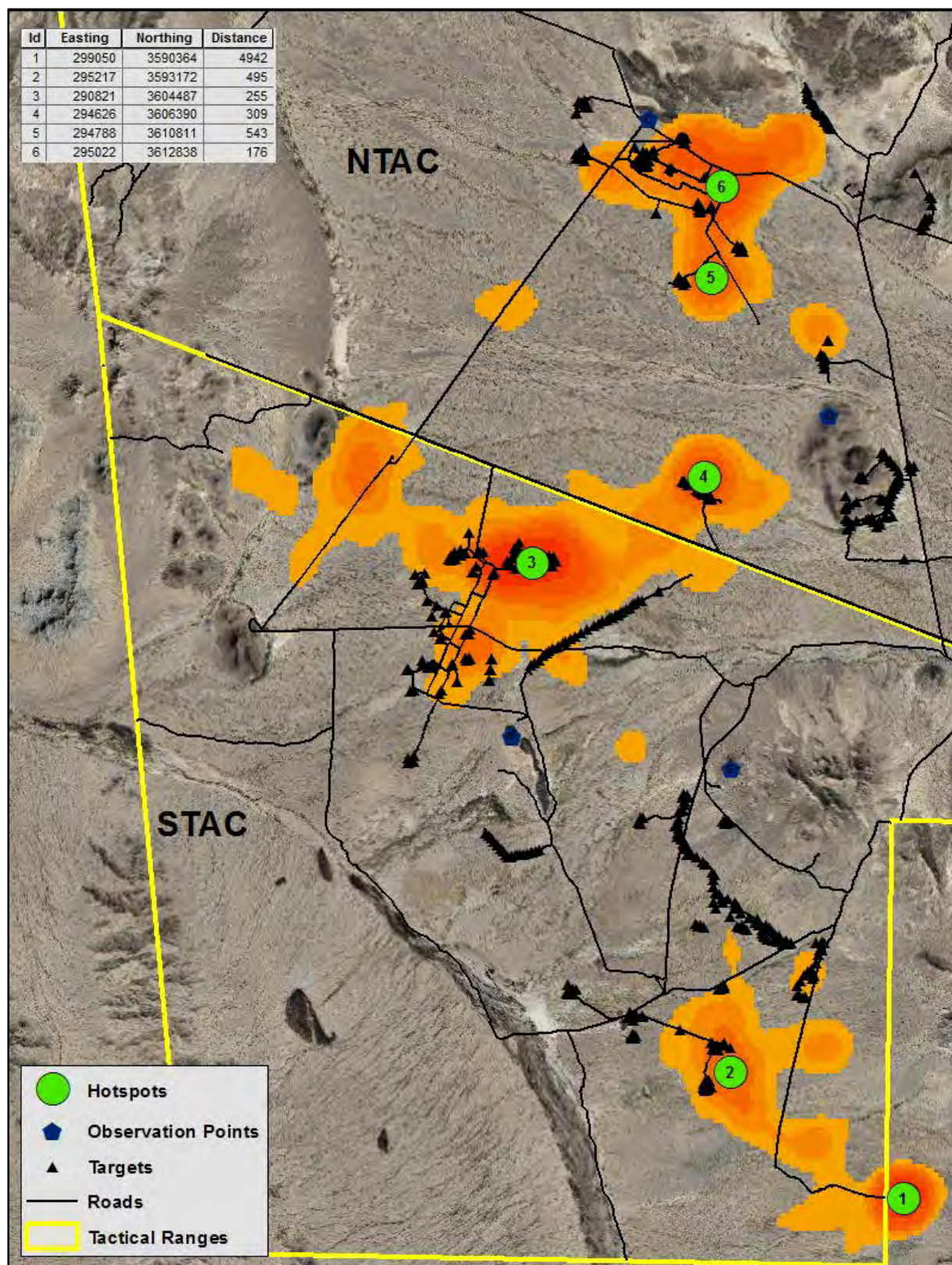


Figure 30 SPH 2010 Summer Season Hotspot Map with Underlying KDE Raster

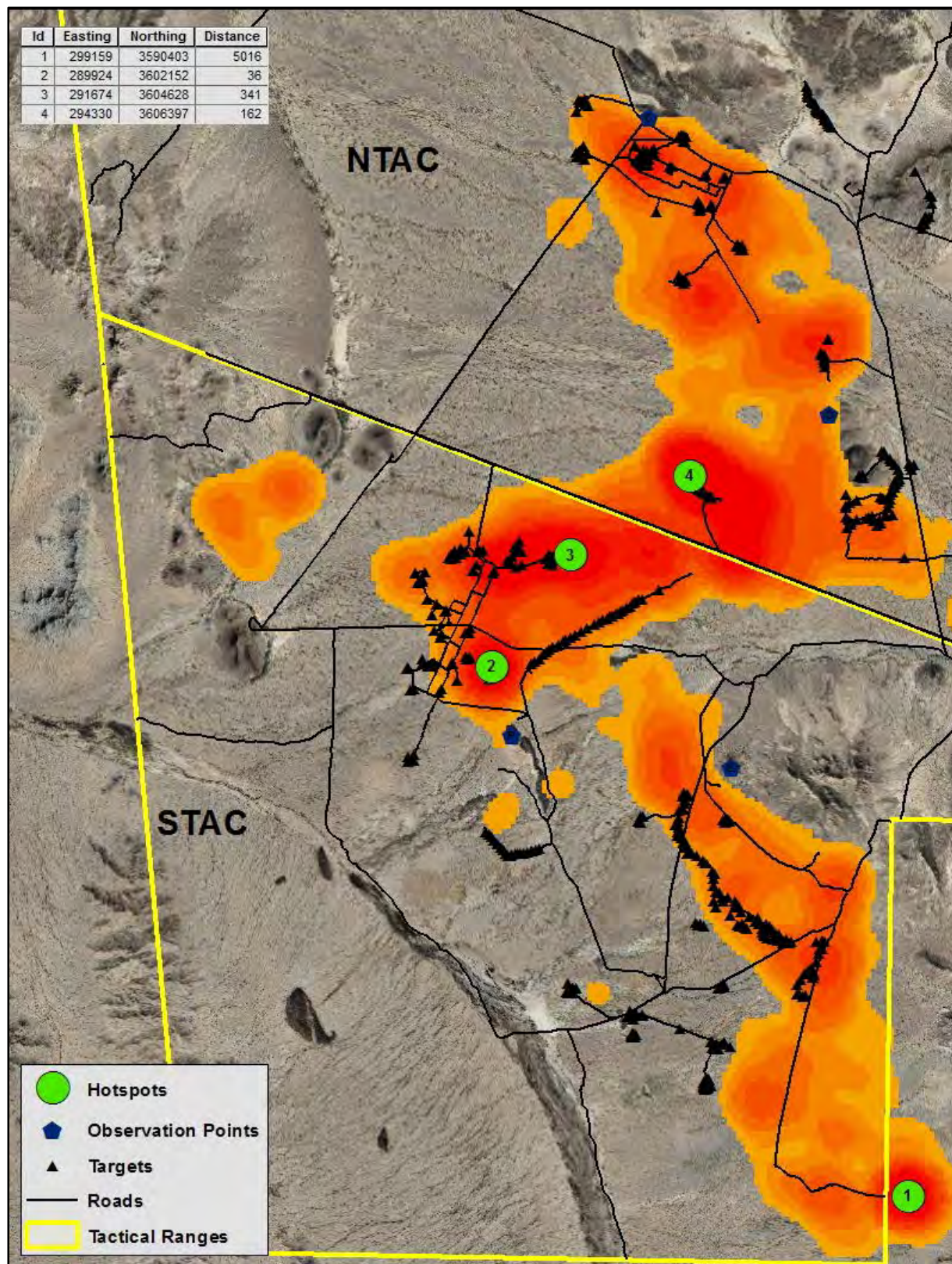


Figure 31 SPH 2011 Hotspot Map with Underlying KDE Raster

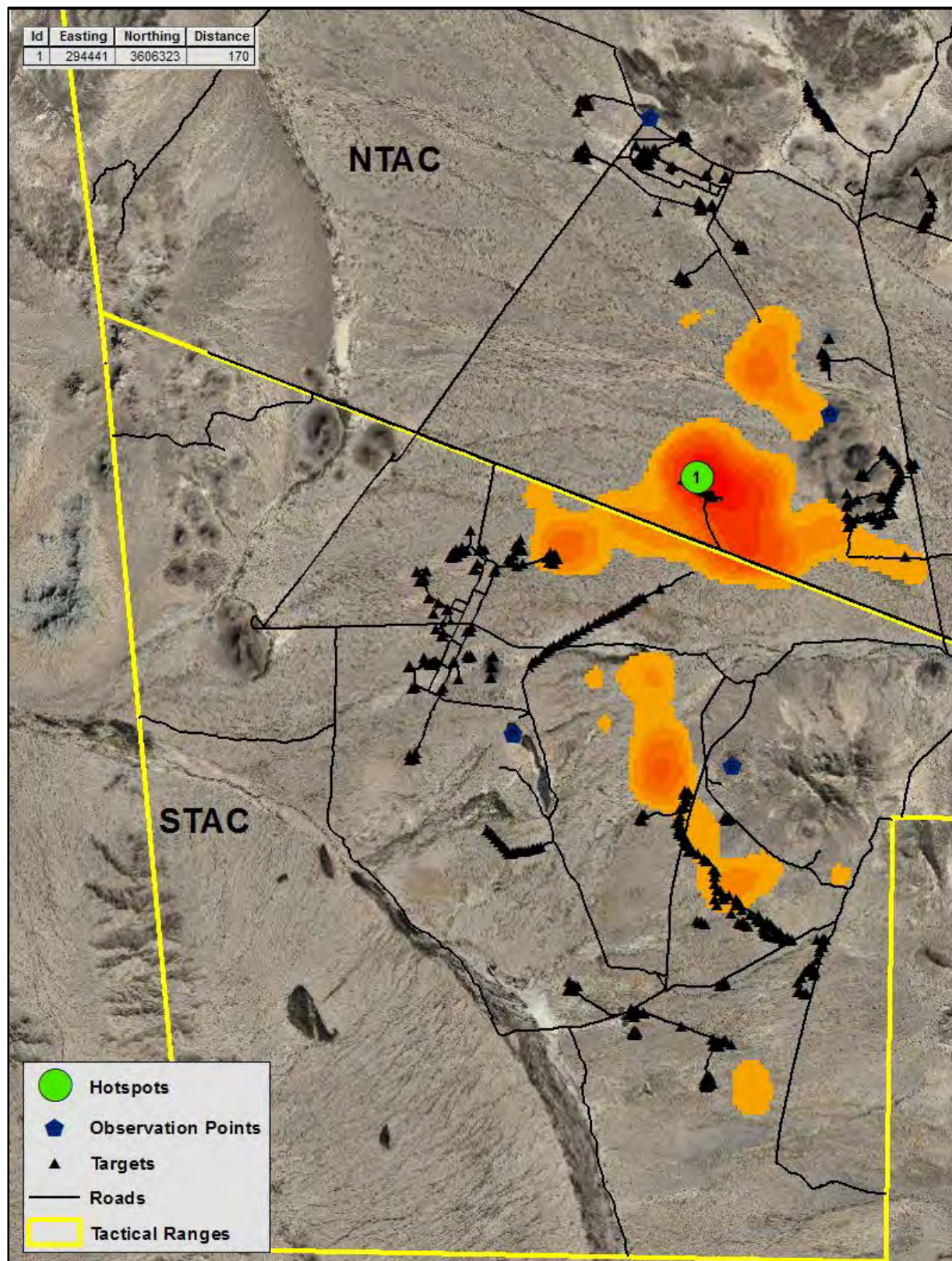


Figure 32 SPH 2011 Breeding Season Hotspot Map with Underlying KDE Raster

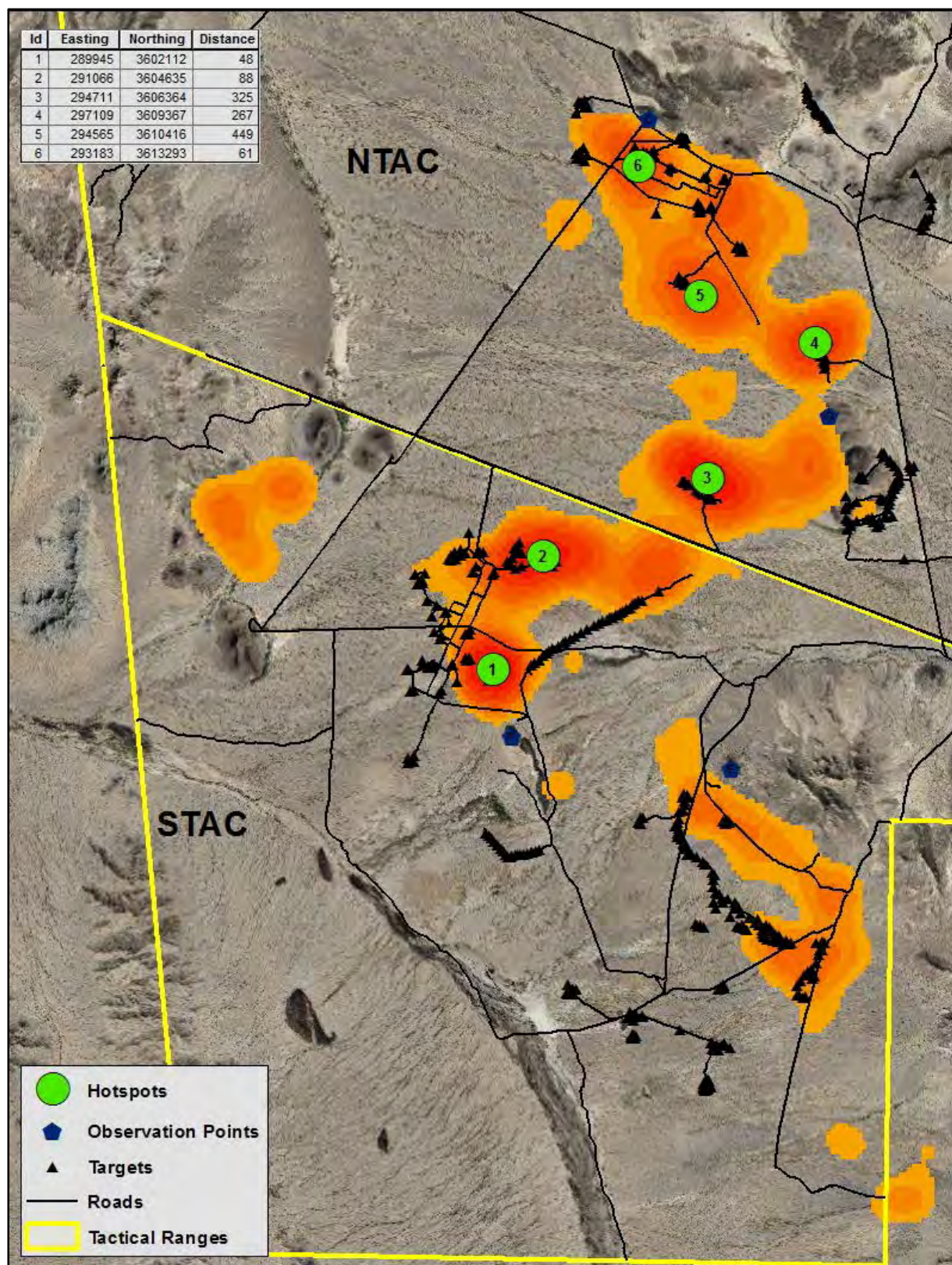


Figure 33 SPH 2011 Fawning Season Hotspot Map with Underlying KDE Raster

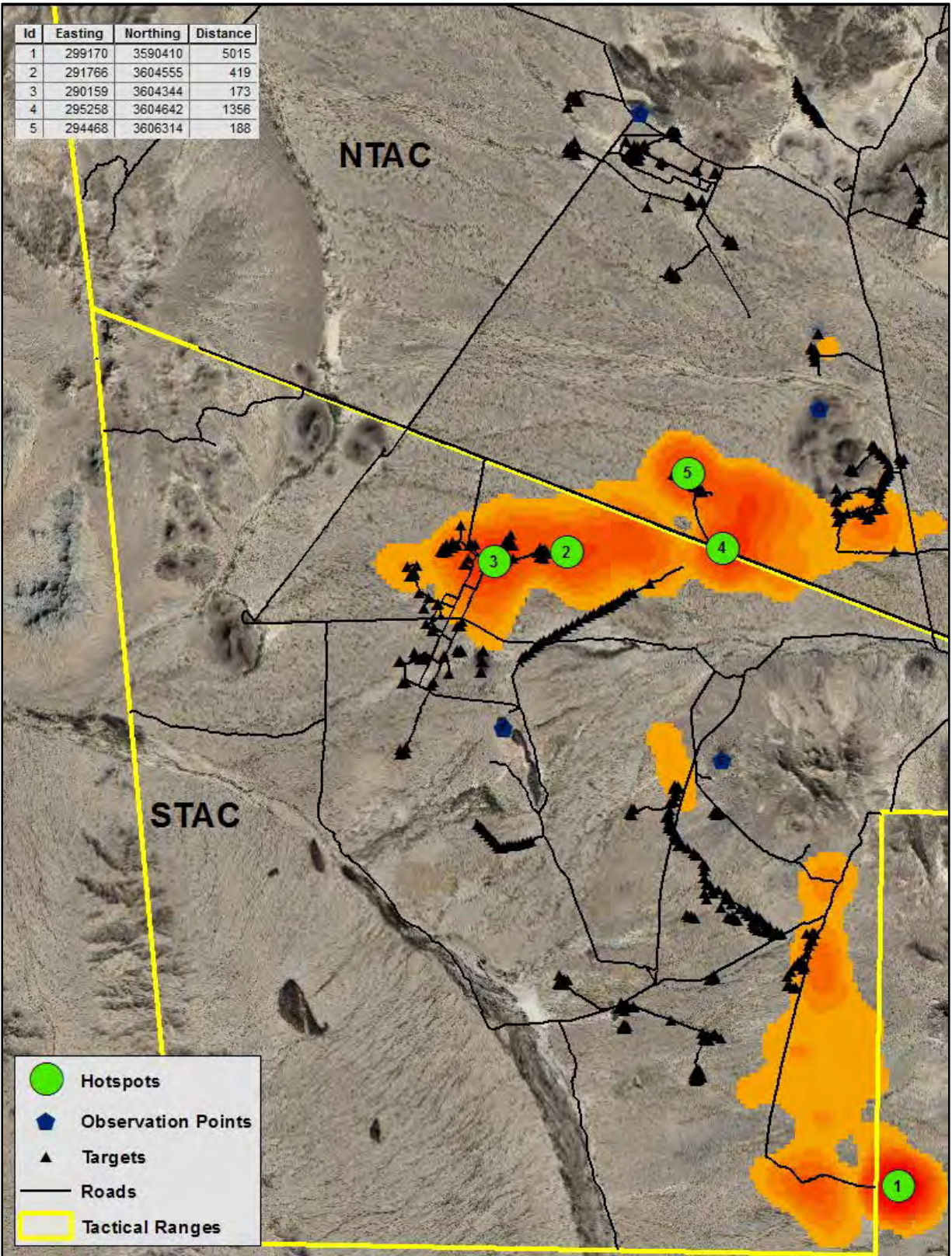


Figure 34 SPH 2011 Summer Season Hotspot Map with Underlying KDE Raster

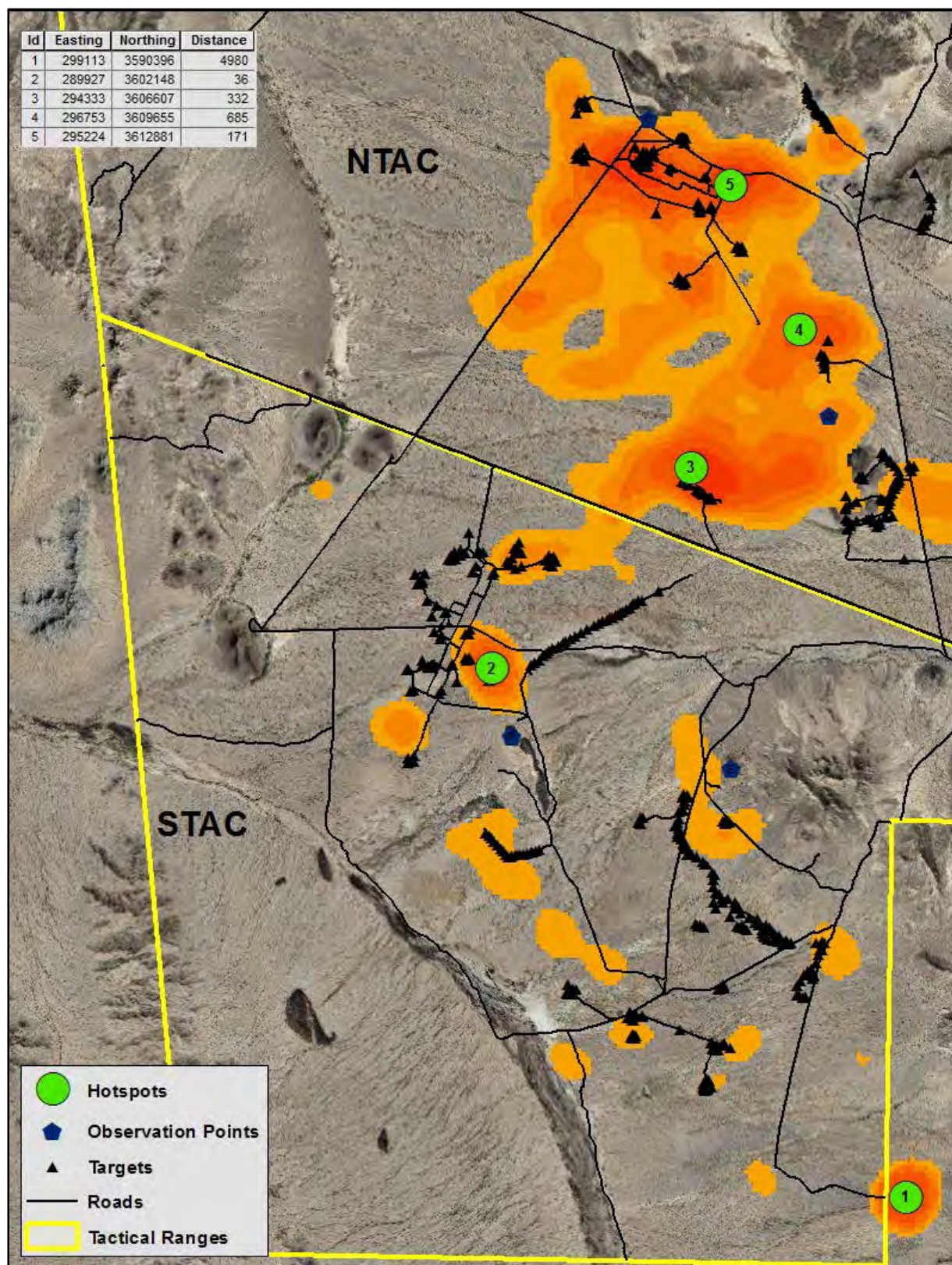


Figure 35 SPH 2012 Hotspot Map with Underlying KDE Raster

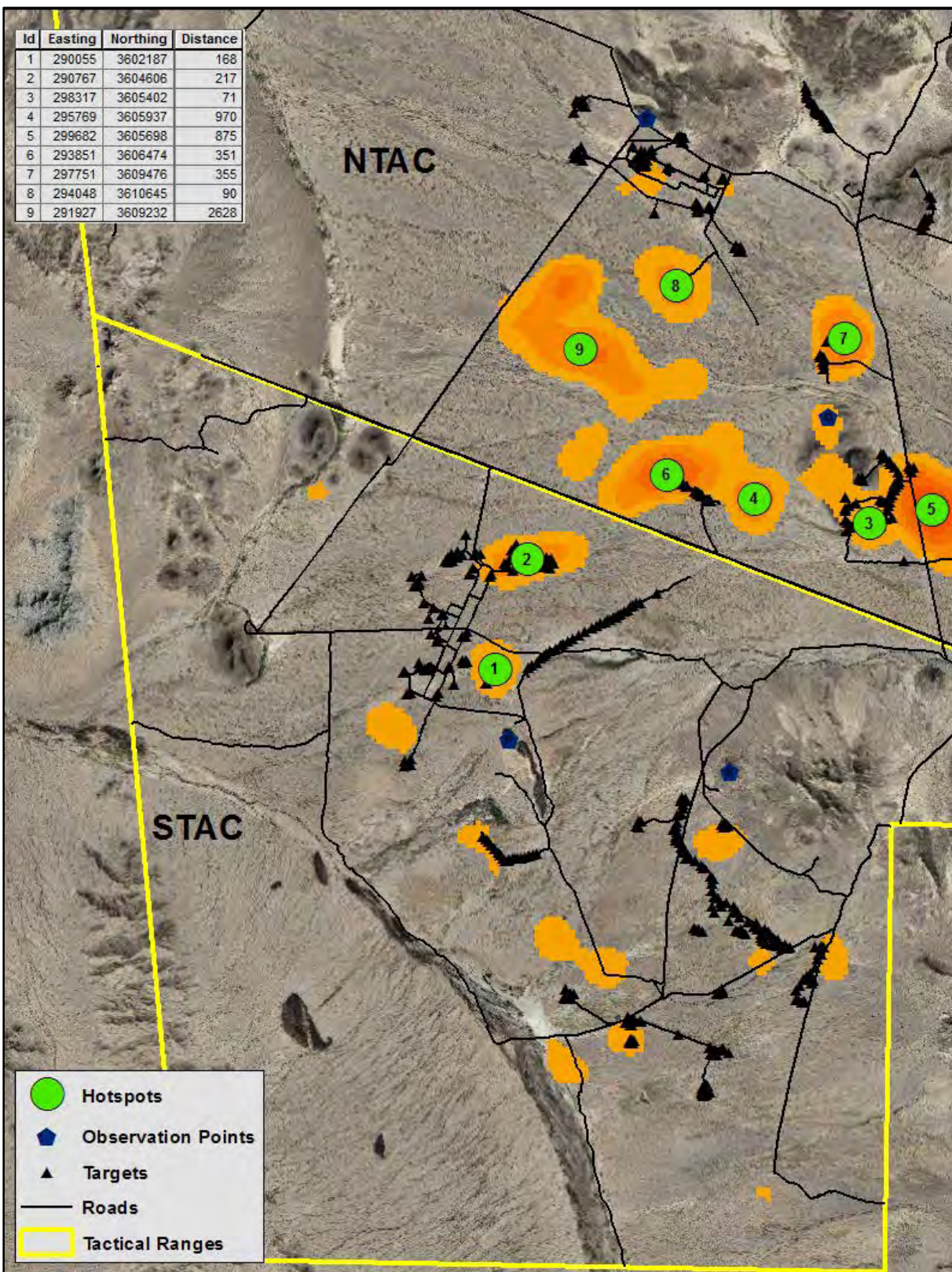


Figure 36 SPH 2012 Breeding Season Hotspot Map with Underlying KDE Raster

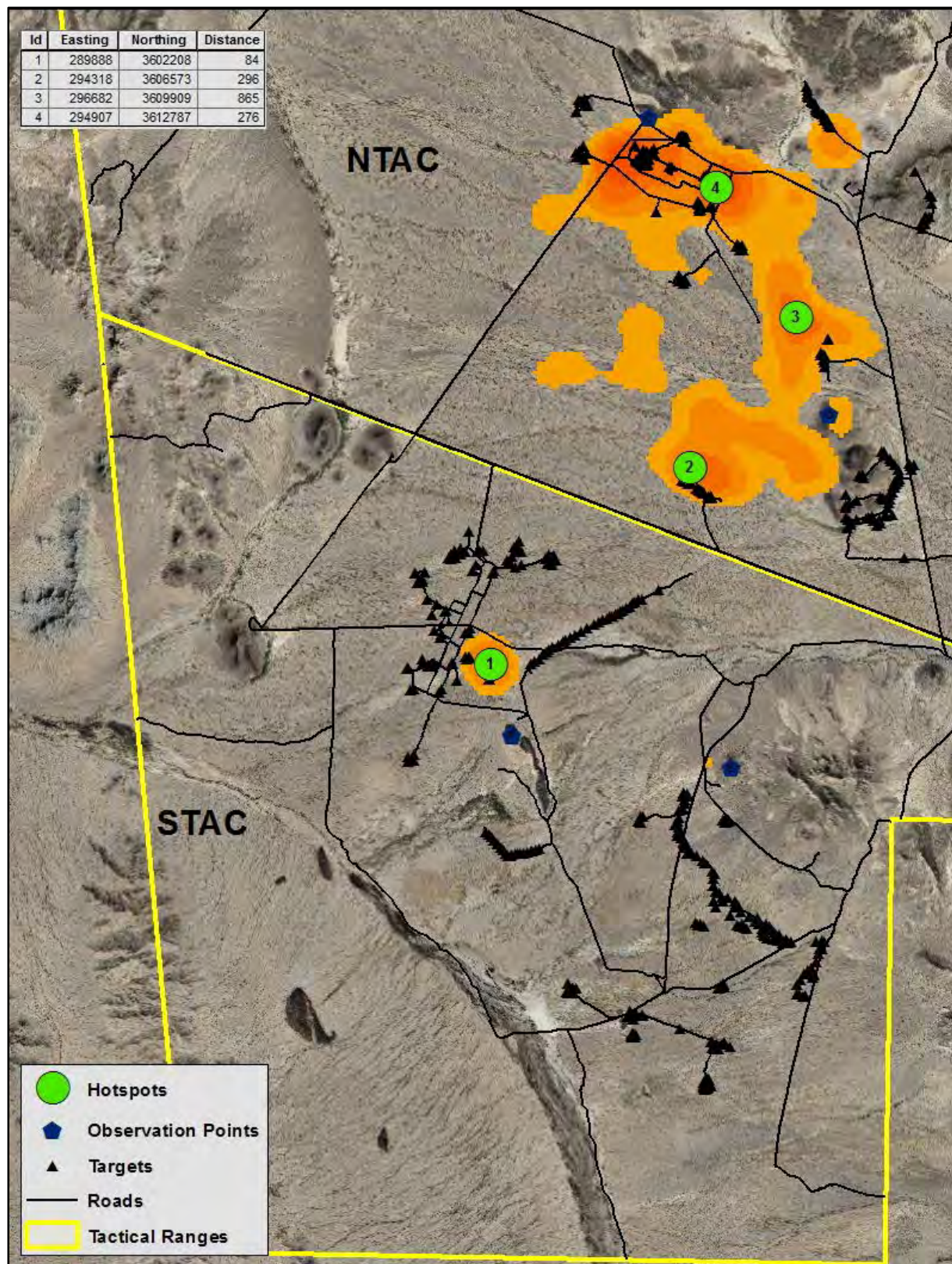


Figure 37 SPH 2012 Fawning Season Hotspot Map with Underlying KDE Raster

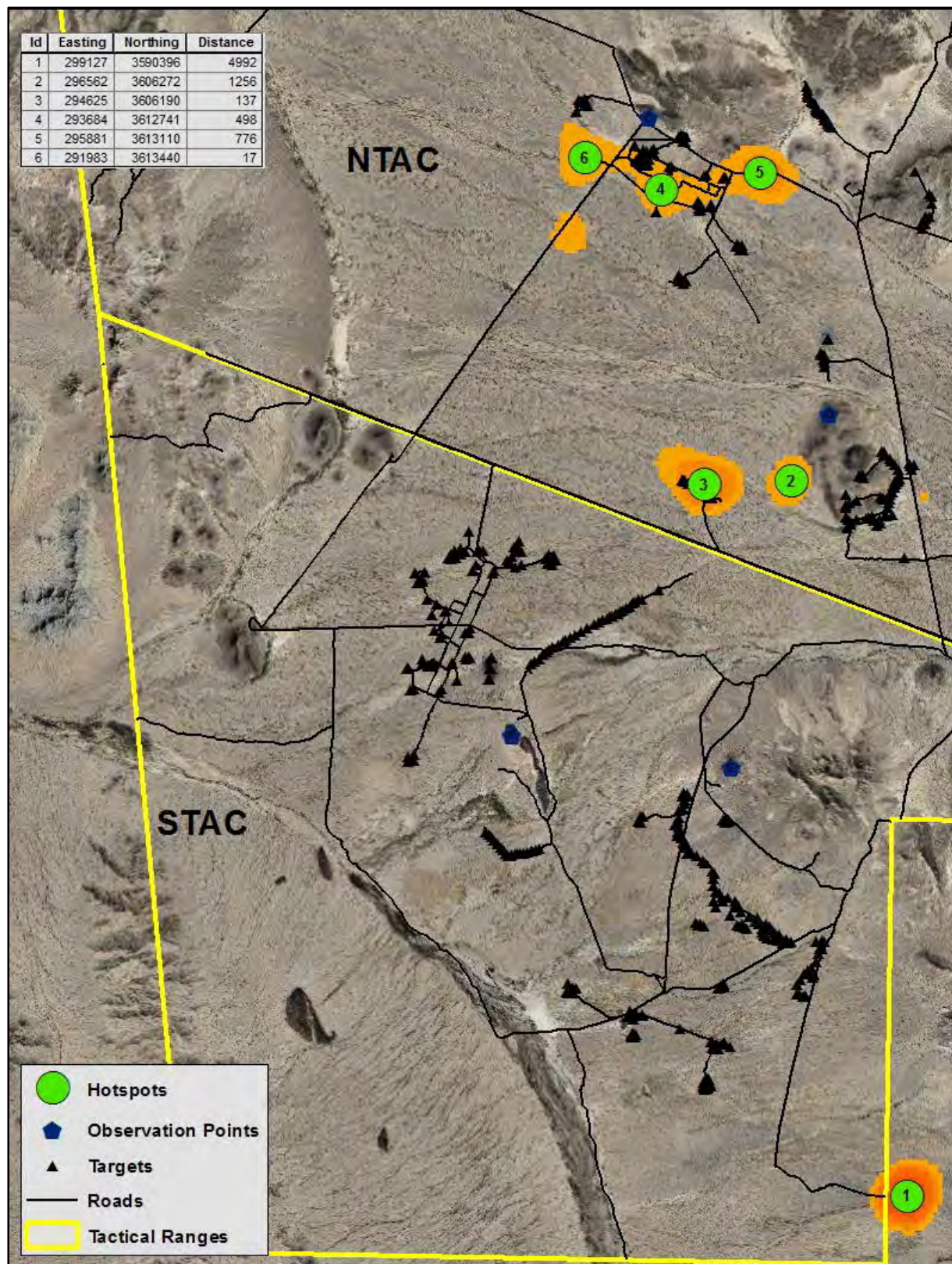


Figure 38 SPH 2012 Summer Season Hotspot Map with Underlying KDE Raster

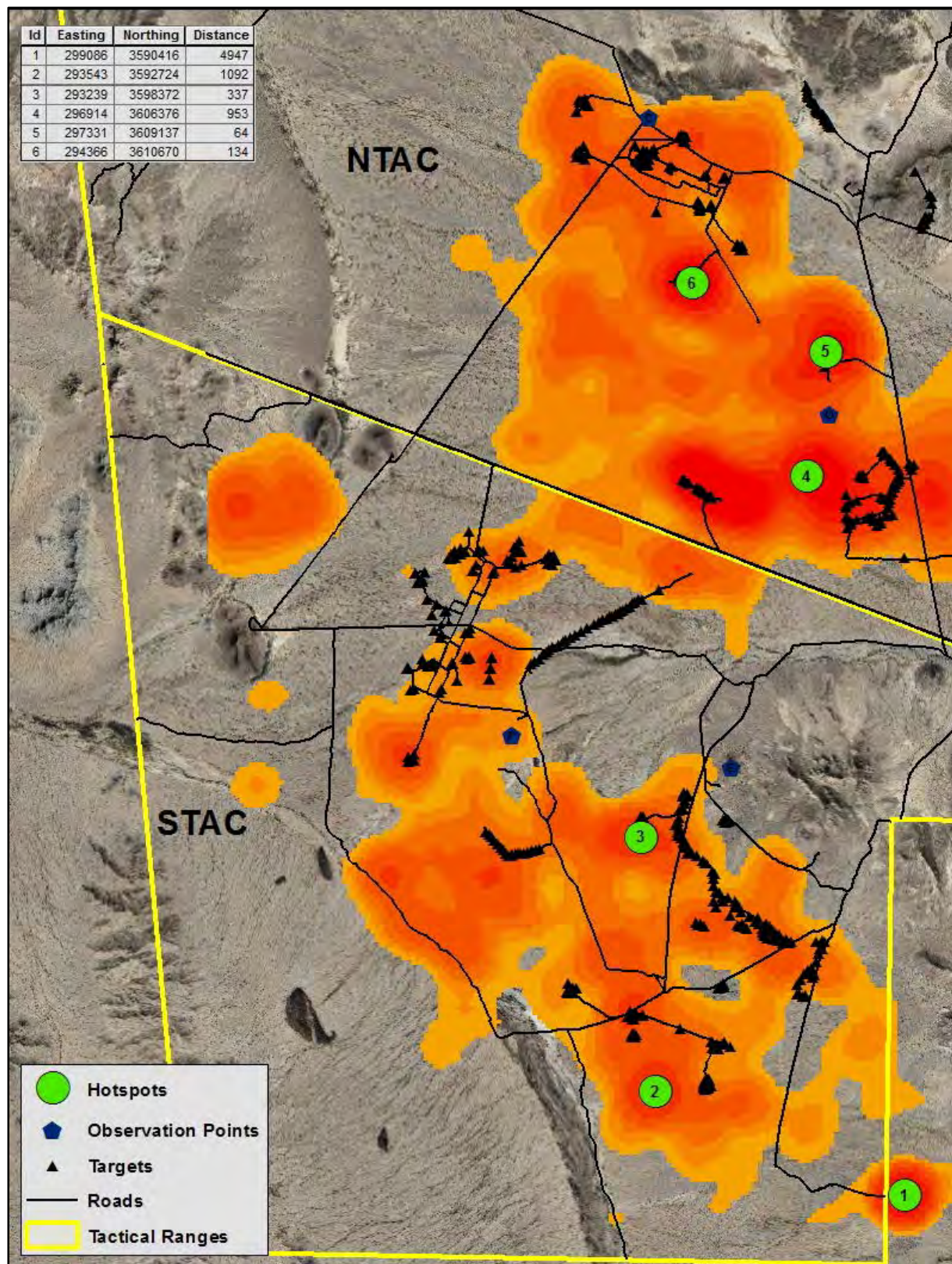


Figure 39 SPH 2013 Hotspot Map with Underlying KDE Raster

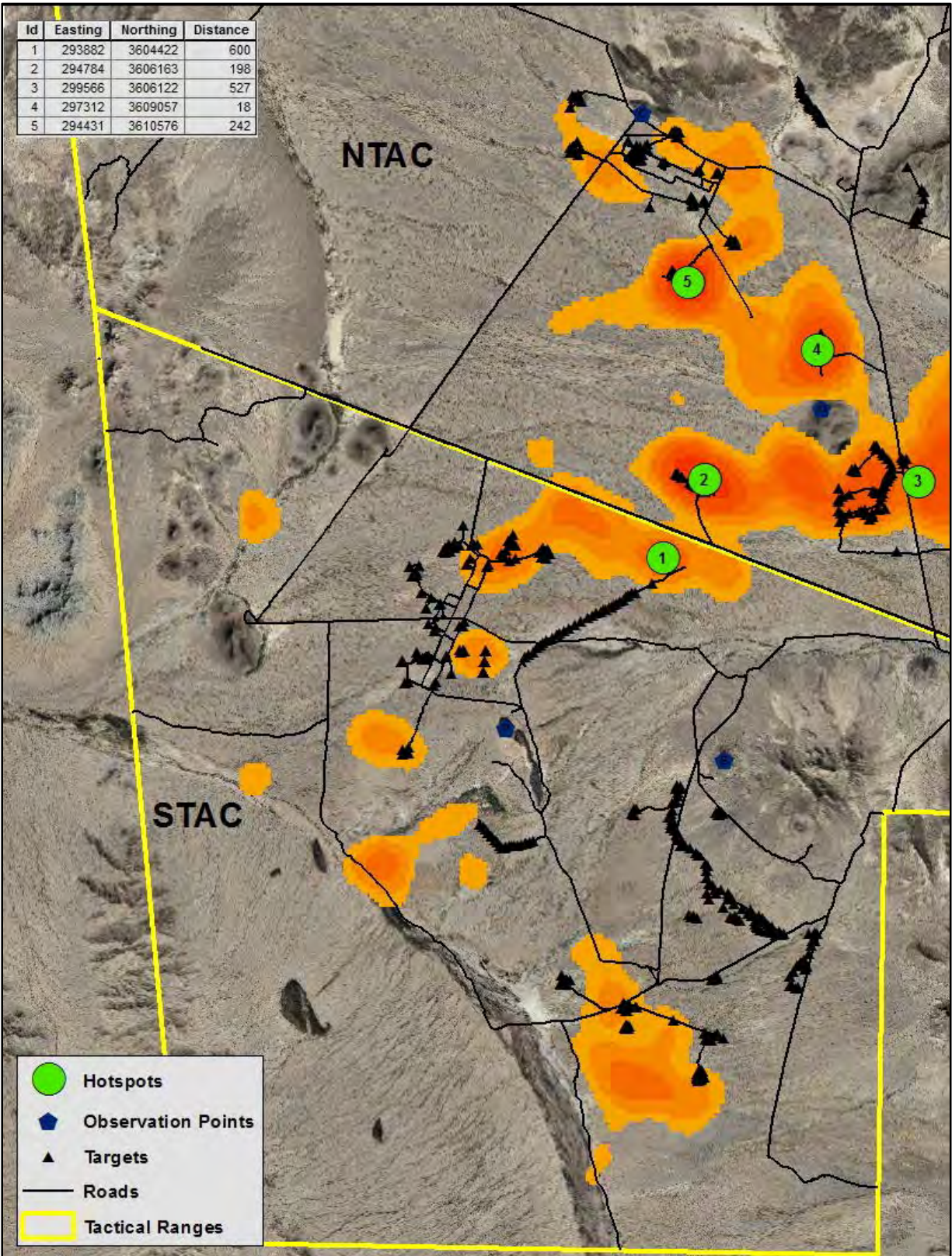


Figure 40 SPH 2013 Breeding Season Hotspot Map with Underlying KDE Raster

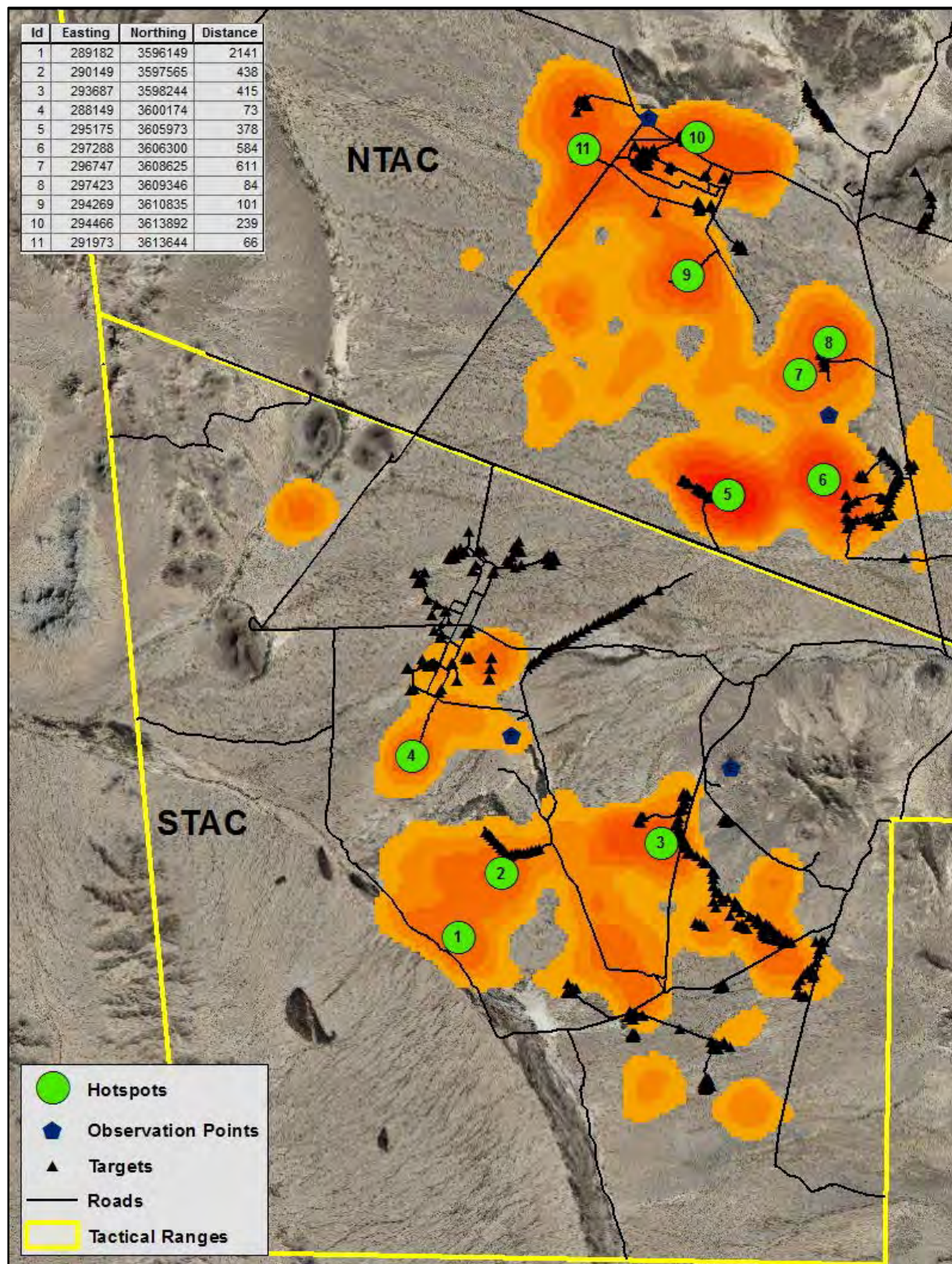


Figure 41 SPH 2013 Fawning Season Hotspot Map with Underlying KDE Raster

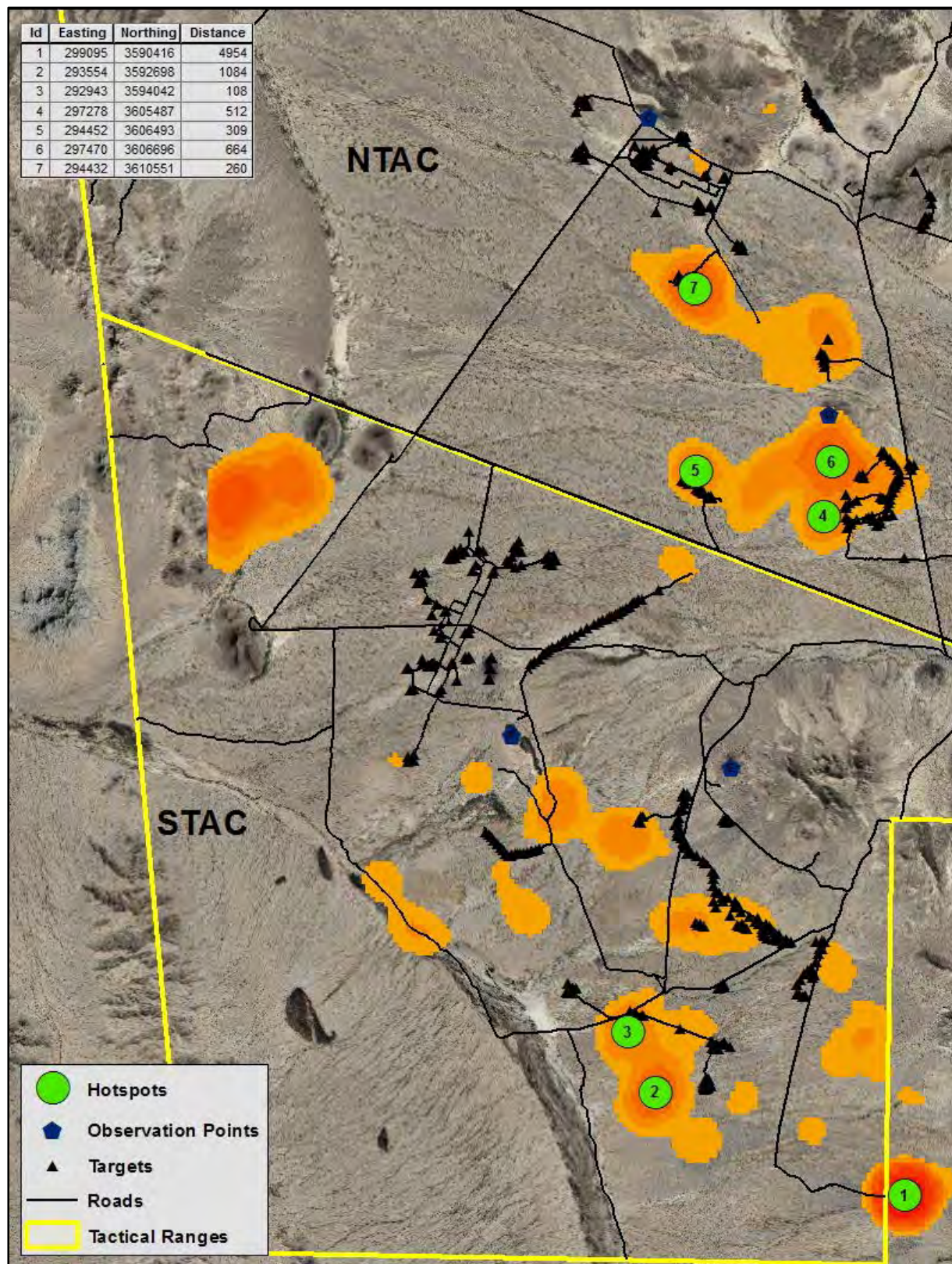


Figure 42 SPH 2013 Summer Season Hotspot Map with Underlying KDE Raster

**APPENDIX B: SEASONAL HOTSPOT DISTANCE TABLE**

**Table 5 Seasonal Hotspots' Distance to Nearest Target**

<u>Year</u>	<u>Season</u>	<u>Hotspot</u>	<u>Distance</u>
2010	breeding	1	66
2010	breeding	2	245
2010	fawning	1	190
2010	fawning	2	640
2010	fawning	3	475
2010	fawning	4	301
2010	summer	1	4942
2010	summer	2	495
2010	summer	3	255
2010	summer	4	309
2010	summer	5	543
2010	summer	6	176
<hr/>			
2011	breeding	1	170
2011	fawning	1	48
2011	fawning	2	88
2011	fawning	3	325
2011	fawning	4	267
2011	fawning	5	449
2011	fawning	6	61
2011	summer	1	5015
2011	summer	2	419
2011	summer	3	173
2011	summer	4	1356
2011	summer	5	188
<hr/>			
2012	breeding	1	168
2012	breeding	2	217
2012	breeding	3	71
2012	breeding	4	970
2012	breeding	5	875
2012	breeding	6	351
2012	breeding	7	355
2012	breeding	8	90
2012	breeding	9	2628
2012	fawning	1	84
2012	fawning	2	296
2012	fawning	3	865
2012	fawning	4	276
2012	summer	1	4992
2012	summer	2	1256
2012	summer	3	137
2012	summer	4	498

2012	summer	5	776
2012	summer	6	17
2013	breeding	1	600
2013	breeding	2	198
2013	breeding	3	527
2013	breeding	4	18
2013	breeding	5	247
2013	fawning	1	2141
2013	fawning	2	438
2013	fawning	3	415
2013	fawning	4	73
2013	fawning	5	378
2013	fawning	6	584
2013	fawning	7	611
2013	fawning	8	84
2013	fawning	9	101
2013	fawning	10	239
2013	fawning	11	66
2013	summer	1	4954
2013	summer	2	1084
2013	summer	3	108
2013	summer	4	512
2013	summer	5	309
2013	summer	6	664
2013	summer	7	260